Research progress on optimized membranes for vanadium redox flow batteries

INORGANIC CHEMISTRY FRONTIERS

REVIEW

View Article Online
View Journal | View Issue

Cite this: *Inorg. Chem. Front.*, 2024, **11**, 4049

Research progress on optimized membranes for vanadium redox flow batteries

Yang Yang,[a] Quge Wang, [a] Shizhao Xiong *[c,d] and Zhongxiao Song*[a,b]

Energy storage systems are considered one of the key components for the large-scale utilization of renewable energy, which usually has an intermittent nature for production. In this case, vanadium redox flow batteries (VRFBs) have emerged as one of the most promising electrochemical energy storage systems for large-scale application, attracting significant attention in recent years. To achieve a high efficiency in VRFBs, the polymer electrolyte membrane between the positive and negative electrodes is expected to effectively transfer protons for internal circuits, and also prevent cross-over of the catholyte and anolyte. However, the high cost of membrane materials is currently a crucial factor restricting the large-scale application of VRFBs. In this review, key aspects related to the polymer electrolyte membranes in VRFBs are summarized, including their functional requirements, characterization methods, transport mechanisms, and classification. According to its classification, the latest research progress on the polymer electrolyte membrane in VRFBs is discussed in each section. Finally, the research directions and development of next-generation membrane materials for VRFBs are proposed, aiming to present a future perspective of this component in full batteries and inspire the ongoing efforts for building high-efficiency VRFBs in the power grid.

Received 27th February 2024,
Accepted 14th May 2024

DOI: 10.1039/d4qi00520a

rsc.li/frontiers-inorganic

1. Introduction

With the increasing energy consumption, it is imperative to develop efficient methods for the production of energy to avoid the depletion of fossil fuels and reduce greenhouse gas emission. In this case, renewable energy sources such as solar and wind energy are abundant and have much lower greenhouse gas emissions and high sustainability compared to fossil fuels. However, their inherent intermittent nature and volatility affect their large-scale integration into the power grid.[1–3] Among the currently developed large-scale energy storage systems, electrochemical energy storage systems have attracted significant attention owing to their advantages such as short construction period and flexible usage scenarios.[4,5] The most widely used lithium-ion batteries (LIBs) have an excellent specific energy and small volume, making them suitable for portable applications; however, their thermal runaway issue poses serious safety risks particularly for large-scale applications.[6,7] Therefore, redox flow batteries have received considerable attention because of their high reliability, fast response time, long lifespan and performance decoupling of capacity and power.[8–10]

As shown in Fig. 1a, a typical redox flow battery system is mainly composed of a core stack, two external storage tanks for storing electrolytes (catholyte and anolyte), pumps for transporting the electrolytes, and liquid flow pipelines. The core stack consists of several repeating units including five main components, *i.e.*, electrodes, membrane, bipolar plates, current collectors, and end plates, as shown in Fig. 1b. In this stack, the polymer electrolyte membrane is one of the critical components because this membrane separates the catholyte from the anolyte during the operation of the flow battery and functions to conduct charge carriers. Moreover, another function of the membrane is to minimize the cross-over of the active materials and prevent short circuits.[9,11,12] Furthermore, the polymer electrolyte membrane should have excellent mechanical and chemical stability to ensure the long-term durability of the battery.[13] Finally, it must be affordable for the economic feasibility and market penetration potential of redox flow battery systems.[11,14]

Among the various flow battery chemistries, the vanadium redox flow battery (VRFB) designed by Skyllas-Kazacos *et al.* presents effective suppression of cross-over of the positive and negative electrolytes because it employs different valence vanadium

[a]*State Key Laboratory for Mechanical Behavior of Materials, Xi'an Jiaotong University, Xi'an, 710049, China. E-mail: zhongxiaosong@mail.xjtu.edu.cn*
[b]*Engineering Research Center of Energy Storage Materials and Devices, Ministry of Education, Xi'an Jiaotong University, Xi'an, 710049, China*
[c]*Faculty of Materials Science and Engineering, Kunming University of Science and Technology, Kunming, 650093, China. E-mail: shizhao.xiong@chalmers.se*
[d]*Department of Physics, Chalmers University of Technology, SE 412 96 Göteborg, Sweden*

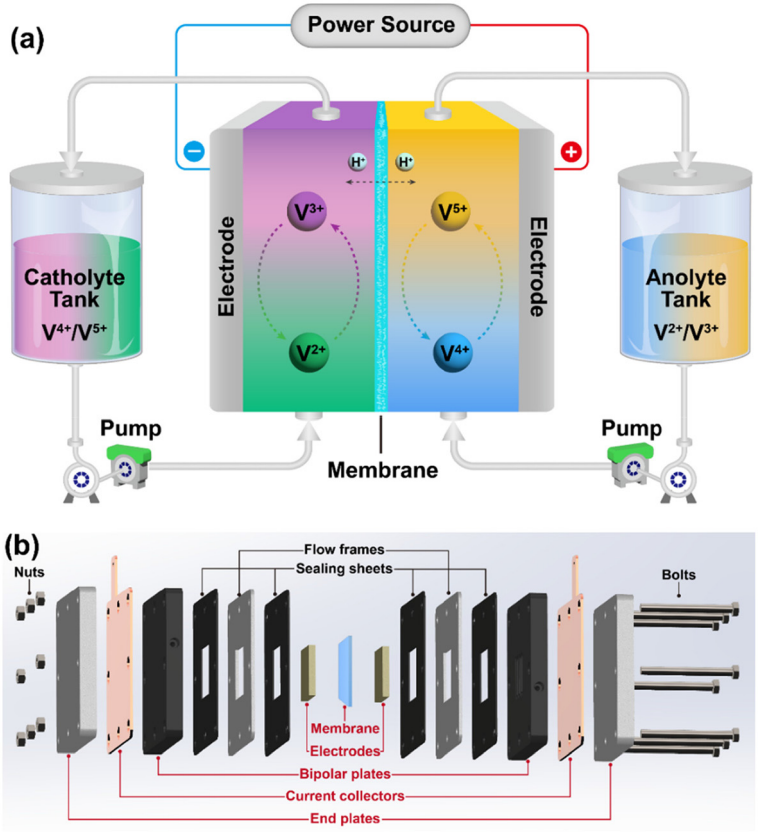

Fig. 1 Schematic diagram of (a) a vanadium redox flow battery (VRFB) system and (b) single cell.

elements in the positive and negative cells to realize redox reactions.[15] Nowadays, VRFB has received continuous and extensive research interest and has been configured in the power grid for output regulation.[16–18] However, VRFB face the same challenge with the polymer electrolyte membrane as other redox flow batteries, including iron-based,[19,20] zinc-based,[21,22] organic-based[23,24] and other novel flow batteries.[25–27] Specifically, only perfluorosulfonic acid proton exchange membranes (Nafion) exhibit excellent stability and proton conductivity at room temperature, but they are expensive and exhibit poor ion selectivity and mechanical properties simultaneously.[8,28–30] Thus, in recent years, tremendous effort has been devoted to the continuous development of polymer electrolyte membranes due to their selectivity, conductivity, stability and reduced cost.

2. Evaluation criteria of membrane

The properties of polymer electrolyte membranes are strongly associated with the performance of full batteries, and thus systematic characterization using standardized evaluation criteria is essential for the comparison of various membranes. As shown in Fig. 2, the evaluation criteria of membranes mainly include water absorption, swelling ratio, ion exchange capacity, ionic selectivity, proton conductivity, mechanical properties, chemical stability, and cost. High-performance vanadium flow batteries with promising development prospects require membranes that exhibit high ionic conductivity, low cross-over of active substances, low solvent absorption, good mechanical and chemical stability and economic feasibility for large-scale applications. In this section, we summarize the key indicators and testing methods of the membrane. In addition, the utilization of polymer electrolyte membranes is discussed, and the electrochemical performance of the full battery is also discussed.

2.1 Water uptake and swelling ratio

Hydrophilic polymer electrolyte membranes usually have a high swelling ratio, which greatly reduces their ionic selectivity. To ensure the reliability of membranes, it is necessary to evaluate their water uptake and swelling ratio. The water uptake rate (WU) of a membrane is defined as the rate of weight change of the wet membrane (immersed in electrolyte) relative to the dry membrane, while the swelling ratio (SR) is defined as the rate of change in length from the dry membrane to the wet membrane. WU and SR can be calculated using the following equations:[31,32]

$$\mathrm{WU} = \frac{W_{\mathrm{wet}} - W_{\mathrm{dry}}}{W_{\mathrm{dry}}} \times 100\% \quad (1)$$

$$\mathrm{SR} = \frac{L_{\mathrm{wet}} - L_{\mathrm{dry}}}{L_{\mathrm{dry}}} \times 100\% \quad (2)$$

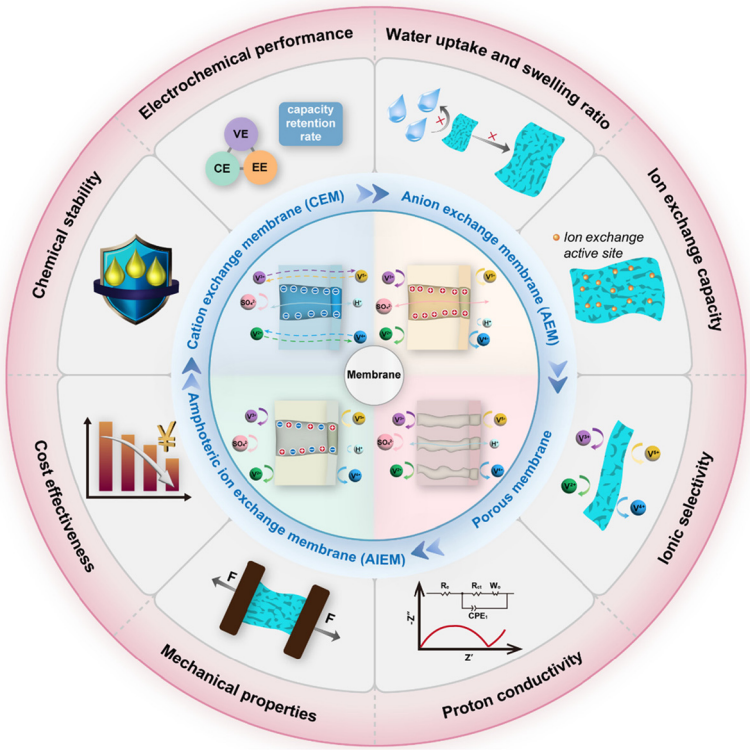

Fig. 2 Schematic of membrane classification, structure, and evaluation criteria of membranes for vanadium redox flow batteries.

where W_{wet} and W_{dry} are the weight of the wet membrane and dry membrane, respectively. L_{wet} and L_{dry} are the length of wet membrane and dry membrane, respectively.

2.2 Ion exchange capacity

During the electrochemical charge–discharge process, charge carriers need to easily pass through the membrane to reduce the Ohmic loss, enabling excellent voltage efficiency and overall battery performance.[33] However, excessive ion exchange capacity (IEC) may aggravate the unwanted crossover of the active materials through the membrane.[12] Therefore, it is necessary to adjust the IEC value to achieve a compromise between the ionic conductivity of the membrane and crossover of the active materials.

The ion exchange capacity of polymer electrolyte membranes can be calculated by back titration.[34–36] In the case of CEM, it is usually soaked in a certain concentration of hydrochloric acid solution to protonate its sulfonic acid groups. Then, it is thoroughly rinsed and soaked in deionized water to remove excess hydrochloric acid. For the titration process, the dried membrane is soaked in an NaCl solution to replace the protons in the sulfonic acid groups with sodium ions. Next, phenolphthalein is used as an indicator to titrate the exchanged H^+ and the value of IEC is calculated using eqn (3), as follows:[36]

$$\mathrm{IEC}(\mathrm{mol\,g^{-1}}) = \frac{C_{\mathrm{NaOH}} \cdot V_{\mathrm{NaOH}}}{W_{\mathrm{d}}} \quad (3)$$

where C_{NaOH} is the concentration of NaOH solution and V_{NaOH} is the volume of NaOH solution consumed in titration. W_d is the weight of the protonated dry membrane.

2.3 Ionic selectivity

During the operation of a flow battery, the osmotic pressure and electric field drive the migration of the active materials through ion-selective membranes, leading to self-discharge and capacity degradation in the battery.[37,38] In asymmetric flow battery systems, such as organic,[39] alkaline zinc iron,[40] and polysulfide[41,42] based redox flow batteries, high ion selectivity is particularly important given that it determines the lifetime of the battery system. In addition, low ion selectivity may also cause membrane fouling during the long-term operation. Taking the Nafion membrane as an example, vanadium ions with low diffusivity (such as VO_2^+ and V^{3+}) deposit on the surfaces of the membrane, while vanadium ions with high diffusivity (such as VO^{2+} and V^{2+}) enter the channels of the membranes and accumulate inside, both of which reduce the ionic conductivity of the membrane and increase the resistance of the battery.[33]

The ionic permeability of vanadium ions is usually measured using an H-shaped permeation cell separated by a membrane, as shown in Fig. 3.[43] Both sides of the tank are filled with an equal volume of $VOSO_4$ and $MgSO_4$ solutions, respectively. The $MgSO_4$ solution is sampled at regular intervals and the concentration of VO^{2+} is measured using a UV

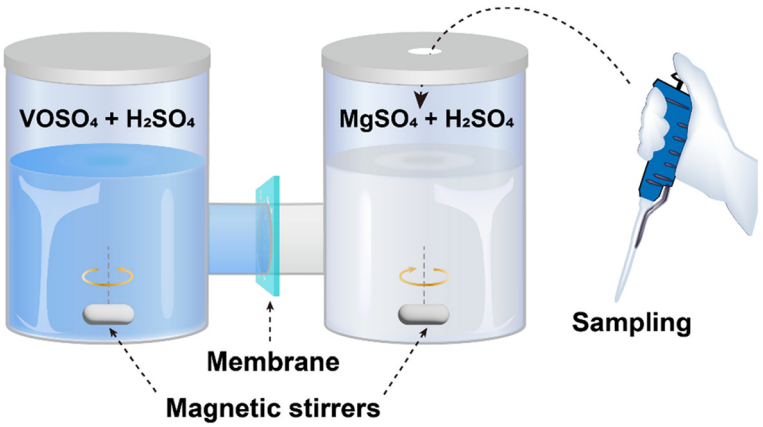

Fig. 3 Schematic diagram of H-type osmotic cell for measuring ion permeability.

visible spectrophotometer. The VO^{2+} permeability (P) can be calculated using eqn (4), as follows:[44,45]

$$V\frac{dC_t}{dt} = \frac{A \cdot P}{L}(C_0 - C_t) \quad (4)$$

where V is the volume of $MgSO_4$ solution, A is the effective area of the membrane, L is the thickness of the membrane, C_0 is the initial concentration of $VOSO_4$, and C_t is the concentration of VO^{2+} in the $MgSO_4$ sampling solution at time t.

There are critical steps in the procedure for the measurement of ionic permeability. (i) The concentrations of the two solutes and the supporting electrolyte must be consistent to maintain similar initial osmotic pressures. (ii) Magnetic stirring should be applied during testing to prevent concentration polarization on the surface of the membrane.[46] (iii) The device must be well sealed to ensure the accuracy of the test results. (iv) The tested solution needs to be refilled to its initial position after each test and it is important to maintain a constant volume of liquid on both sides.

2.4 Proton conductivity

During the cycling of a redox flow battery, the energy barriers at the interface between the electrolyte and polymer membrane, as well as inside the membrane increases the Ohmic polarization and energy loss. As the key objectives of redox flow batteries, high power density and high voltage efficiency require a low internal resistance, which is dependent on the proton conductivity of the polymer membrane.[47]

Electrochemical impedance spectroscopy (EIS) is the common method employed to evaluate the proton conductivity (σ) of membranes.[48,49] The use of the same cell device and electrolyte composition as that in the conventional redox flow battery provides a more realistic evaluation.[50,51] The resistance of the cell device is tested with and without a membrane and the proton conductivity (σ) of the membrane can be calculated using eqn (5), as follows:[52]

$$\sigma(\mathrm{S\,cm^{-1}}) = \frac{L}{A(R_1 - R_2)} \quad (5)$$

where L is the thickness of the membrane, A is the effective area of the membrane, and R_1 and R_2 are the resistance with and without the membrane, respectively.

2.5 Mechanical properties

During the long-term operation of a redox flow battery, the membrane is required to have excellent mechanical strength to resist changes in the battery pressure, which is especially important for solid mixed redox flow batteries. For instance, the membrane of a zinc-based redox flow battery needs sufficient mechanical strength to reduce the risk of penetration by zinc dendrites and further short circuit of the battery.[53,54]

The characterization of the mechanical properties is mainly carried out using a tensile testing machine. In the case of Nafion membranes, it is essential to test both wet and dry samples.[55,56] The tensile strength can be calculated using eqn (6), as follows:[57]

$$T = \frac{F_m}{W \cdot L} \quad (6)$$

where T refers to the tensile strength of the membrane, F_m is the maximum tensile stress, W is the width of the sample, and L is the thickness of the membrane.

2.6 Chemical stability

Redox flow battery systems generally use strong acid or alkali as the supporting electrolyte, and their internal components are also immersed in an environment of strong oxidizing or reducing active materials during their operation.[58–61] Therefore, the membrane need to possess good chemical stability to suppress its corrosion and degradation in harsh environments, ensuring the stable cycling of the battery.

The chemical stability of membranes is usually tested by *ex situ* methods.[62,63] For example, the membrane is soaked in a sulfuric acid solution containing VO^{2+} for 1–3 months after cutting into an equal size shape. Then, it is taken out for comprehensive inspection including macroscopic and microscopic

morphological changes, chemical structure changes, and ion concentration changes in the soaking solution.[45]

2.7 Cost effectiveness

In VRFB, the cost of the ion selective membrane accounts for about 20% of the total system cost,[64] while the cost of the membrane increases to about 38% in iron chromium redox flow batteries.[65] Through the cost analysis of redox flow battery systems, it is considered that the cost of the membrane and electrolyte is an important factor hindering their wide application, and thus developing cost-effective and sustainable ion-selective membranes is crucial.[19,66,67]

2.8 Electrochemical battery performance

The influence of the membrane on the performance of VRFB can be evaluated using the typical electrochemical testing methods for battery systems. Usually, a constant current charge–discharge procedure is used to obtain the cycling performance and voltage profile of the battery. In a flow battery, an ideal polymer electrolyte membrane is expected to provide a high and stable charge–discharge capacity, low charge voltage, and high discharge voltage.[12]

The coulombic efficiency, voltage efficiency, and energy efficiency are the three important indicators to evaluate the battery performance.[68] The coulombic efficiency is a performance indicator to evaluate the ratio of discharge capacity to charge capacity, and a high coulombic efficiency requires a membrane with good resistance to crossover of vanadium species. The voltage efficiency is an indicator for evaluating the overpotential losses during the charge–discharge processes, and a high voltage efficiency is attributed to the excellent ion conductivity of the membrane and the low internal resistance of the battery.[69,70] Energy efficiency is obtained from the product of the coulombic efficiency and voltage efficiency, which represents the overall performance of the battery system. These indicators can be calculated using the following equations:[71]

$$\mathrm{CE} = \frac{\int_0^{t_d} I_d(t)\mathrm{d}t}{\int_0^{t_c} I_c(t)\mathrm{d}t} \times 100\% \quad (7)$$

$$\mathrm{VE} = \frac{\int_0^{t_d} U_d(t)\mathrm{d}t}{\int_0^{t_c} U_d(t)\mathrm{d}t} \times 100\% \quad (8)$$

$$\mathrm{EE} = \mathrm{CE} \times \mathrm{VE} = \frac{\int_0^{t_d} U_d(t)\mathrm{d}t \cdot I_d(t)\mathrm{d}t}{\int_0^{t_c} U_d(t)\mathrm{d}t \cdot I_c(t)\mathrm{d}t} \times 100\% \quad (9)$$

where t_d and t_c denote the discharge time and a charge time of the battery, respectively. I_d and I_c denote the current during charge and discharge of the battery, respectively. U_d and U_c denote the voltage during charge and discharge of the battery, respectively.

The limitation of polarization loss becomes more remarkable during the operation of VRFB under an increasing working current density, which is unfavorable for miniaturization and cost reduction of the battery system. A rate capability test can be performed to evaluate the charge–discharge performance of the battery at different current densities and the discharge capacity, coulombic efficiency, voltage efficiency and energy efficiency are observed during the testing process.[12] Extra attention should be given to the discharge capacity and efficiencies under a high current density, which are crucial in practical applications.[19]

In addition, the cycling stability of a battery is also a key indicator to evaluate the membrane performance. The capacity loss caused by self-discharge during long-term operation can be recovered by remixing the electrolyte.[28] However, the irreversible capacity loss caused by side reactions and liquid leakage will lead to the continuous deterioration of the battery performance.[72] During the cycling of VRFB at a fixed current density, the ratio of the discharge capacity over different cycles can be measured and the capacity retention rate can be calculated.[73]

3. Membrane classification

There are various types of VRFB membranes, which can be divided into two categories of charged membranes and non-charged membranes according to whether ion exchange groups are present in the membranes, as seen in Fig. 2. The charged ion exchange membrane is composed of polymer chains, which have attached functional ion groups. They are formed of fixed ions and dissociated ions (counter ions) with opposite charges.[11] Regarding the charge of the ions dissociated by the functional groups, ion exchange membranes can be divided into cation exchange membranes (CEM), anion exchange membranes (AEM), and amphoteric ion exchange membranes (AIEM). CEMs contain functional groups with a negative charge, such as $-SO_3^-$, $-COO^-$, and $-PO_3^-$, which dissociate H^+. AEMs contain functional groups with positive charge, such as $-NH^{3+}$, $-NRH^{2+}$, and $-NR_2H^+$, which can transport OH^-.[74] AIEMs contain two functional groups distributed in the same polymer matrix. In addition, non-charged membranes are made of membrane materials with lower polarity such as polysulfone, polyethersulfone, and polyvinylidene fluoride, which have better solvent resistance and dimensional stability compared to charged membranes.[75]

The mass transfer of charged membranes usually relies on the dissolution/diffusion mechanism, which is related to the charged ion exchange groups in the membrane. CEMs and AEMs allow the ions that are the same as that in membranes to pass through them and repel dissimilar charge ions. Furthermore, the ions diffuse through the membrane by the interaction of ion exchange groups and pores, and their directional transport is the result of osmotic pressure and an external electric field.[76] Non-charged membranes are usually made with a porous structure to realize the capability of transporting charge carriers, and their selective permeability mainly depends on the screening mechanism. The pore size of non-charged membranes is a prerequisite for ion transfer in the membrane. The hydrated ions can migrate from one side of the membrane to the other along the channels in the membrane when their radius is smaller than that of the pores.[77,78]

4. Crossover of vanadium ions

During the operation of VRFB, proton transport within the membrane is mainly achieved through two modes, media transport and the Grotthuss mechanism.[79] Besides proton transport, transmembrane transport of vanadium ions in VRFB occurs during the charge and discharge processes. As shown in Table 1, the unwanted transmembrane transport of vanadium ions can trigger a series of self-discharge reactions,[80,81] which have a negative influence on the capacity and lifetime of VRFB. The main driving force for the transmembrane transport of vanadium ions is a concentration gradient and electric field.

Mohammadi *et al.* conducted early research on water migration in various commercial ion exchange membranes, and found that water migration occurred from the positive electrode to the negative electrode in the VRFB equipped with AEMs, whereas that equipped with CEMs exhibited water migration in the opposite direction.[82] In addition, the diffusion coefficients of vanadium ions in Nafion 115 follow the order of V^{2+} > VO^{2+} > VO_2^+ > V^{3+}. The transport of vanadium ions and protons is often carried out in the form of bound water and its amount is dependent on the type of ions. As shown in Fig. 4a, each V^{2+} or V^{3+} is connected to 6 bound water molecules, while VO^{2+} is linked to 5 bound water molecules. VO_2^+ is connected to 4 bound water molecules and protons are connected to 2.5 bound water molecules.[80,81] The migration of vanadium ions is driven by the concentration gradient of vanadium ions between the positive and negative electrodes.[83]

In the case of the self-discharge reaction, water transfer is caused by the migration of bound water with vanadium ions and protons, and the permeation (approximately 75%). In the process of charge–discharge, the migration of protons to form internal circuits and the migration of bound water also play a crucial role in the water transfer process. However, the migration of vanadium ions with bound water and their permeation are the main reasons for water transfer during long-term cycling. As shown in Fig. 4b and c, the electrolyte imbalance is enhanced with an increase in the operation time, leading to the severe degradation of the capacity and output performance for VRFB.[80]

Skyllas-Kazacos *et al.* also highlighted that different charge states will also affect the direction of water migration.[82] VRFB equipped with CEM exhibits water migration from the negative electrode to the positive electrode in a high charge state (SOC = 50%–100%), while the opposite direction is observed in the low charge state (SOC = 0%–50%). Moreover, the water migration is more severe in the low charge state compared to that in the high charge state.

The influence of an external electric field on the transmembrane migration of vanadium ions or water also needs to be considered during the operation of a liquid flow battery. Luo *et al.* found that the presence of an electric field accelerates the transmembrane migration of vanadium ions from the positive electrode to the negative electrode during the charge process and inhibits this migration in the reversed direction.[76]

Table 1 Self-discharge reactions in a vanadium redox flow battery (VRFB)

In positive electrode	In negative electrode
$2VO_2^+ + V^{2+} + 2H^+ \rightarrow 3VO^{2+} + H_2O$	$V^{2+} + VO^{2+} + 2H^+ \rightarrow 2V^{3+} + H_2O$
$VO_2^+ + V^{3+} \rightarrow 2VO^{2+}$	$2V^{2+} + VO^{2+} + 4H^+ \rightarrow 3V^{3+} + 2H_2O$
$V^{2+} + VO^{2+} + 2H^+ \rightarrow 2V^{3+} + H_2O$	$VO_2^+ + V^{3+} \rightarrow 2VO^{2+}$

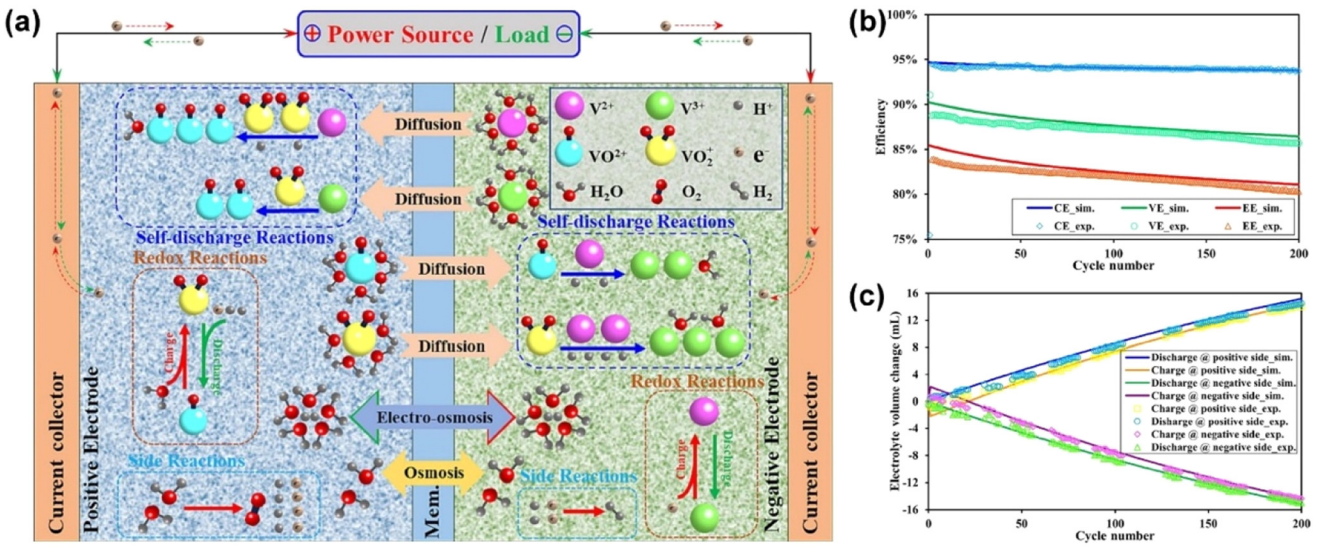

Fig. 4 (a) Illustration of chemical reactions, species crossover and water transport in VRFB. (b) Comparison of the coulombic efficiency, voltage efficiency and energy efficiency of VRFB. (c) Simulation and experimental results of electrolyte volume changes in the catholyte and anolyte tanks after each cycle. Reproduced from ref. 80 with permission from Elsevier, Copyright 2023.

Furthermore, the effect of an electric field on the migration of vanadium ions will be reversed during the discharge process. The migration coefficient of vanadium ions under the action of an electric field follows the order of $VO^{2+} > V^{2+} > V^{3+} > VO_2^+$, and the migration effect caused by an electric field is three orders of magnitude greater than that from a concentration gradient.[76]

5. Nafion-based cation exchange membranes (CEMs)

CEMs are the most developed and widely used membranes in redox flow battery systems. Anionic functional groups, such as $-SO_3^-$, $-COO^-$, and $-PO_3^-$, are immobilized on the main polymer chain, resulting in a relatively high migration rate for protons and other cations. This section focuses on the latest developments of typical Nafion-based membranes in the large-scale application of VRFB.

5.1 Pure perfluorosulfonic acid membranes

Nafion was first developed by DuPont. The chemical structure and its cluster-network model are shown in Fig. 5a.[84] Nafion membranes are thermally and chemically stable, and they have been widely used in the chlor-alkali production industry, energy storage and conversion systems.[85,86] Their excellent chemical stability in various environments, such as acidic, oxidation, and reduction, enables their application in VRFB systems with high concentration of sulfuric acid. The utilization of Nafion membranes is beneficial for the implementation of a high acid concentration in VRFB, thereby enhancing the solubility of the vanadium active materials and the conductivity of the electrolyte.[70] In addition, the integration of a polytetrafluoroethylene (PTFE) backbone with sulfonic acid functional groups in polymer membranes can endow them with hydrophobicity and hydrophilicity (as shown in Fig. 5b), ensuring the high chemical and mechanical strength of the membrane for application in VRFB.

However, Nafion membranes exhibit very low selectivity towards cations, leading to severe crossover of vanadium ions. Also, the resulting migration of bound water aggravates the imbalance in electrolyte volume on the positive and negative sides, reducing the lifespan of the battery.[76,83] In addition, the high cost of Nafion membranes also hinders the further application of redox flow batteries. Thus, extensive effort has been devoted to addressing the above-mentioned issues and novel strategies such as the addition of inorganic and organic components have been proposed.

5.2 Nafion-based inorganic composite membranes

5.2.1 Modification with inorganic nanoparticles. As shown in Fig. 6a, utilizing the shielding effect of inorganic nanoparticles, which are embedded into a polymer matrix, can reduce the permeability of vanadium ions and improve ion selectivity of Nafion based membranes. It is necessary to consider two main factors for material selection, cost and stability. Typical selection of inorganic nanoparticles includes silicon dioxide (SiO_2), titanium dioxide (TiO_2) and tungsten trioxide (WO_3).[88–90]

Xi *et al.* doped SiO_2 in Nafion and obtained a Nafion/SiO_2 hybrid membrane with ion exchange capacity and proton conductivity similar to Nafion117.[90] However, the incorporation of nanoparticles in the channels of Nafion membranes not only inhibits the permeation of vanadium ions, but also reduces the conductivity of protons, resulting in a significant voltage and energy loss in the battery.

Therefore, it is an advanced strategy to prepare composite membranes with functionalized nanoparticles, which are mixed with the polymer solution before the formation of the membrane. Nanoparticles with hydrophilic groups, such as hydroxyl, amino and sulfonic acid groups, can provide intense pathways for proton transport and promote the ionic conductivity.[91] Lin *et al.* prepared Nafion/amino silica composite membranes *via* the sol–gel method, as shown in Fig. 6b.[92] The results of the potentiometric titration and self-discharge tests showed that the exchange capacity of vanadium ions through

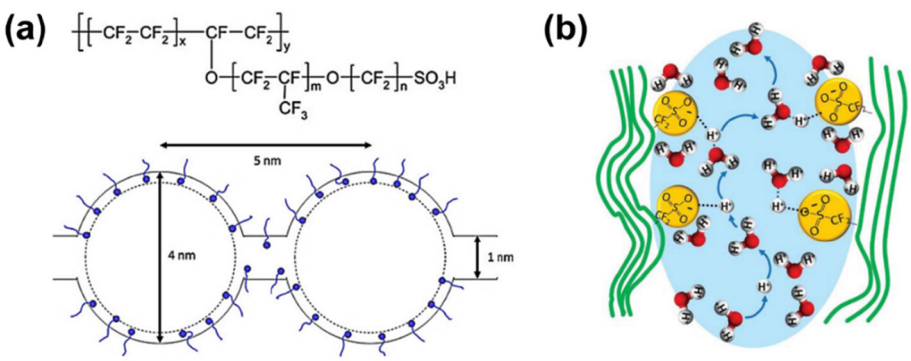

Fig. 5 (a) Structure of Nafion and the cluster-network model. Hydrophilic clusters are connected by short narrow channels. Short curves represent Nafion side chains and dots represent sulfonic acid groups. Reproduced from ref. 84 with permission from Elsevier, Copyright 1983. (b) Proton conduction mechanism in hydrophilic region of hydrated proton exchange membrane. Reproduced from ref. 87 with permission from John Wiley and Sons, Copyright 2023.

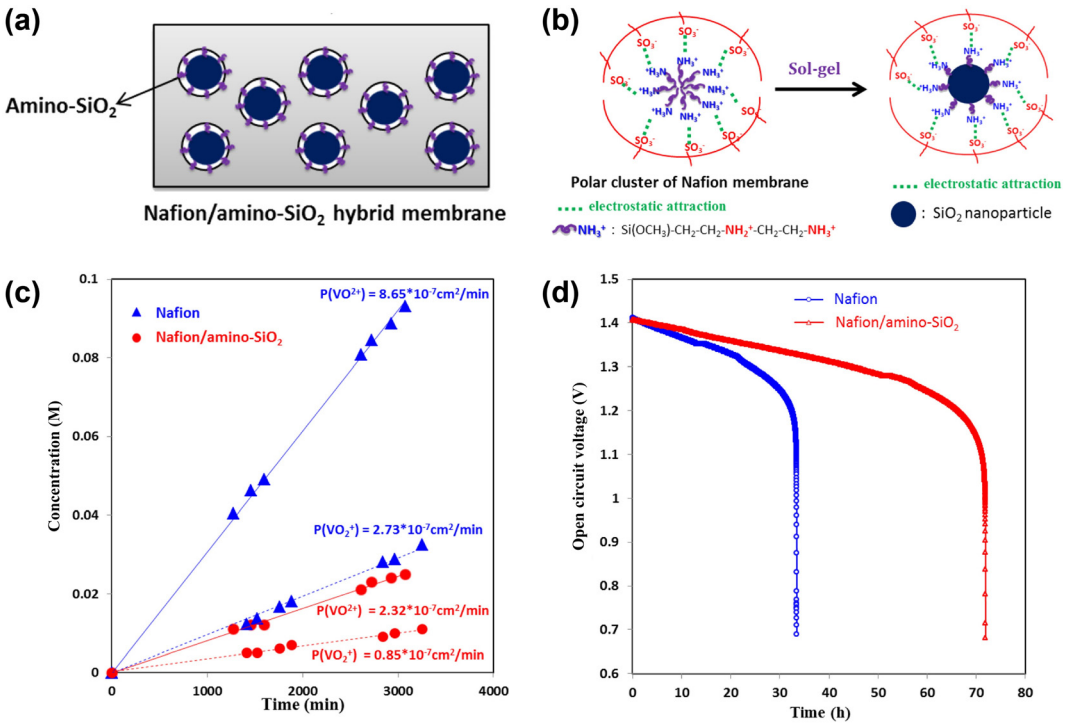

Fig. 6 (a) Schematic illustration of Nafion/inorganic hybrid membrane. (b) Preparation of Nafion/amino-SiO_2 hybrid membrane. (c) Effect of Nafion and Nafion/amino-SiO_2 membrane on intracellular VO^{2+} and VO_2^+ concentration. (d) OCV of VRFB over time using Nafion and Nafion/amino-SiO_2 membrane in the charged state of 75%. Reproduced from ref. 92 with permission from Elsevier, Copyright 2015.

the hybrid membrane is only 26.8% of that in the original Nafion membrane. Fig. 6c and d suggest that the self-discharge rate of the battery was also greatly reduced, and Teng *et al.* reported the similar results.[93,94]

5.2.2 Modification with inorganic nanowires/nanotubes. The above-mentioned inorganic nanoparticles/Nafion composite membranes are effective to reduce vanadium ion permeation and improve ion selectivity. However, nanoparticles with a high specific surface area tend to agglomerate, leading to a decrease in the membrane stability and accelerating the penetration rate of vanadium ions.[95] Therefore, inorganic nanowires/nanotubes have been introduced to modify ion exchange membranes.

Aziz *et al.* prepared ZrO_2 nanotubes (ZrNT) with a diameter of less than 50 nm and incorporated them in Nafion to prepare a Nafion/ZrNT composite membrane *via* the solution casting method.[95] Two-dimensional inorganic nanofillers serve as barriers to the permeation of vanadium ion, delivering a significant increase in ion selectivity. Similarly, Ye *et al.* prepared a Nafion/TiO_2 nanotube composite membrane (Fig. 7a–c).[73] The super-hydrophilic TiO_2 nanotubes significantly inhibited the permeability of vanadium ions without a decrease in proton conductivity. The battery with the composite membrane maintained 55.7% discharge capacity after 1400 cycles (Fig. 7d), while the battery using commercial Nafion membrane could only deliver 20% discharge capacity after 410 cycles. Aziz *et al.* further mixed TiO_2 and ZrO_2 nanotubes to prepare a Nafion/$TiZrO_4$NT composite membrane (Fig. 7e). The Nafion/$TiZrO_4$NT composite membrane exhibited excellent proton conductivity (75.9 mS cm^{-1}) and impressive ion selectivity (3.61×10^6 S min cm^{-3}) at room temperature. This proves the superiority of inorganic co-doping in membrane materials for high-performance redox flow batteries.[96]

5.2.3 Modification of inorganic nanosheets. Besides solution casting, spin coating is another common method to modify polymer membranes and the direct coating of nanoparticles on the surface of the membrane can form an even barrier layer, hindering the permeation of vanadium ions (Fig. 8a and b). Furthermore, the utilization of nanosheets with a large transverse size can significantly improve the permeation blocking efficiency (Fig. 8c). The typical nanosheet materials include graphene oxide (GO)[55] and graphite nitride carbon (g-C_3N_4).[97] Zhang *et al.*[98] successfully constructed a composite membrane with an enhanced interface, which consisted of cross-linked graphene oxide (CLGO), as shown in Fig. 8d. The cross-linked GO layer and angstrom-scale channels significantly reduced the vanadium ion permeability, and the composite membrane showed good mechanical and chemical stability, improving the electrochemical performance of the assembled battery.

5.3 Nafion-based organic composite membranes

Based on the bonding between the organic components and Nafion polymer matrix, Nafion-based organic composite membranes can be classified as covalent-modified membranes and non-covalent-modified membranes. There are two typical con-

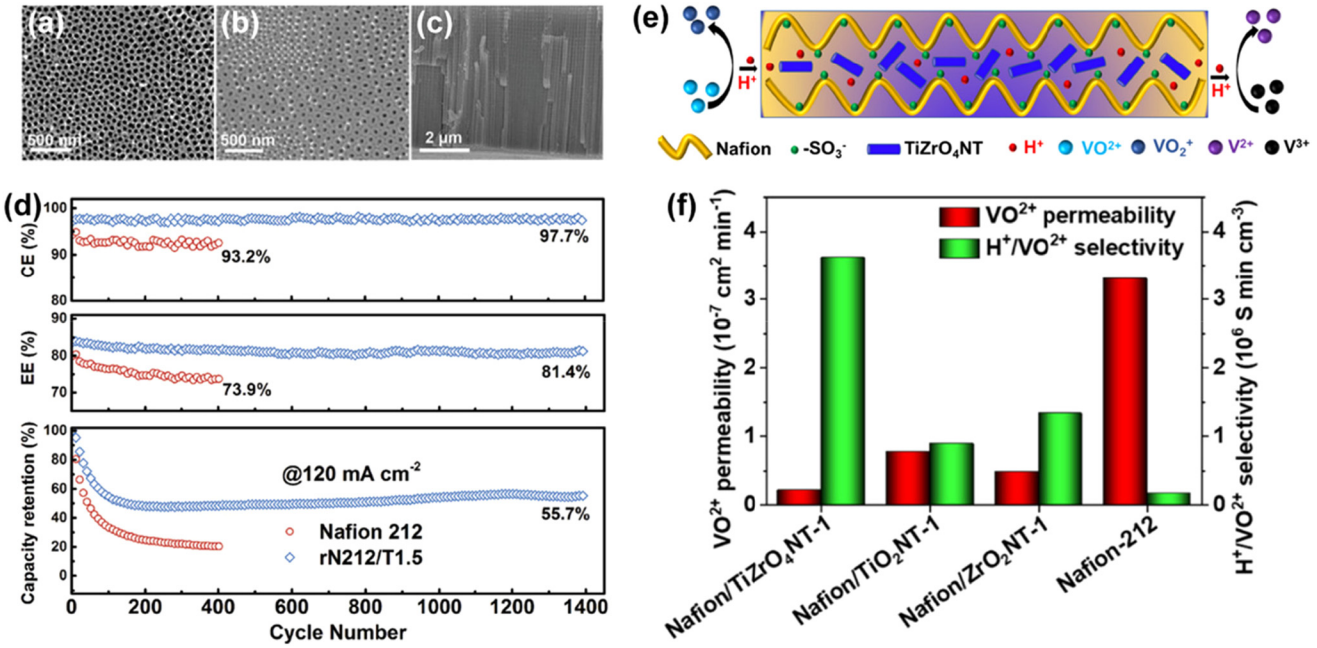

Fig. 7 (a) Top, (b) bottom and (c) cross-sectional SEM images of TiO_2 nanotube arrays. (d) Coulombic efficiency, energy efficiency and discharge capacity retention of VRFB single cells with Nafion and Nafion/TiO_2 membrane for cycling at 120 mA cm^{-2}. Reproduced from ref. 73 with permission from John Wiley and Sons, Copyright 2020. (e) Schematic diagram of proton transfer and vanadium ion diffusion mechanism in the fabricated Nafion/$TiZrO_4$NT composite membrane. (f) VO^{2+} permeability and H^+/VO^{2+} selectivity of the Nafion and composite membrane. Reproduced from ref. 96 with permission from the American Chemical Society, Copyright 2021.

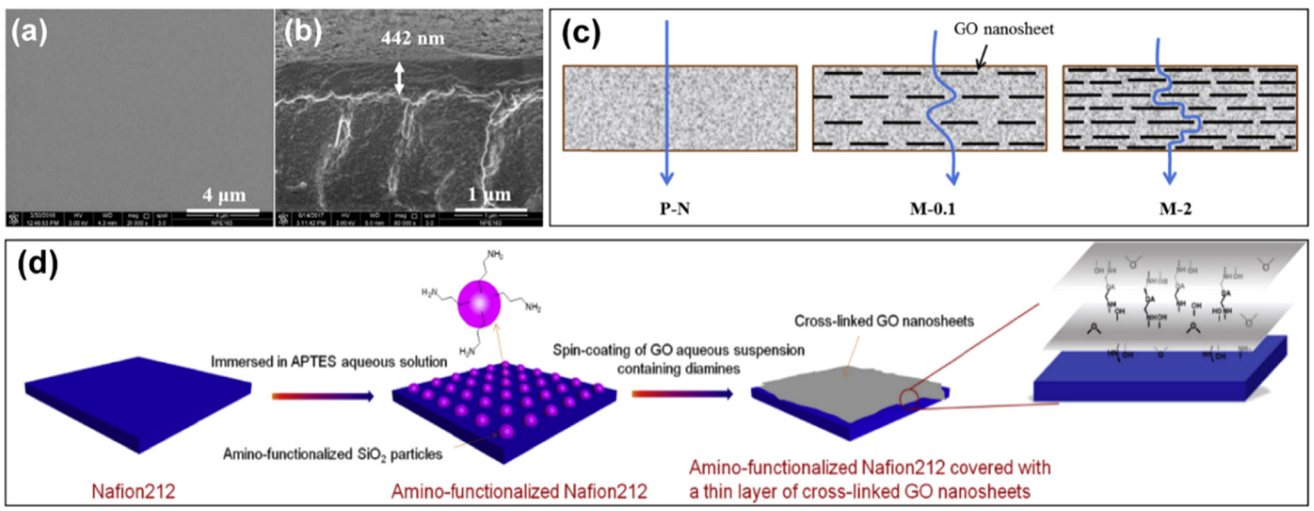

Fig. 8 SEM images of (a) surface and (b) cross-section of graphene oxide/Nafion membrane. (c) Schematic diagram of permeation of vanadium ions in pure Nafion and graphene oxide/Nafion composite membrane. Reproduced from ref. 55 with permission from Elsevier, Copyright 2017. (d) Process for the preparation of amino-functionalized Nafion212 covered with graphene oxide nanosheets. Reproduced from ref. 98 with permission from Elsevier, Copyright 2019.

figurations, the sandwich structure and blending organic components with Nafion. Between them, the sandwich structure is composed of a Nafion inner layer sandwiched by organic surface layers. The performance of this type of composite membrane is synergistically improved by the excellent chemical stability and high ion conductivity of the Nafion layer, as well as the high ion selectivity of the surface layer. Alternatively, blending composite membranes are fabricated *via* the direct mixing of organic materials with Nafion.

5.3.1 Covalently modified composite membranes. Covalently modified composite membranes form a functional layer through the chemical reaction between the modified components and the Nafion membrane, effectively reducing the permeation of vanadium ions and improving the ion

selectivity and chemical stability of the membrane. Luo *et al.* introduced a polyethylene imine (PEI) layer on the surface of a Nafion membrane by interface polymerization.[99] Due to the presence of a large number of amino groups in PEI, the vanadium ion permeability of the composite membrane significantly decreased due to its positive charge repulsion effect. Similarly, Ma *et al.* grafted copolymerized *N*,*N*-dimethylaminoethyl methacrylate (DMAEMA) on a Nafion substrate through radiation induction and protonated it to reduce the crossover of vanadium ion (as shown in Fig. 9a).[100] Dai *et al.* used surface-initiated atom transfer radical polymerization (SI-ATRP) technology to graft zwitterionic sulfobetaine methacrylate (SBMA) on Nafion to form a composite membrane (N115-*g*-PSBMA).[101] The amphoteric layer of the N115-*g*-PSBMA membrane had low vanadium permeability and the VRFB assembled with this membrane showed high coulombic efficiency and energy efficiency.

It is worth noting that the dense surface layer formed by covalent modification can significantly reduce the vanadium ion permeability, water absorption and water migration in the membrane, but it inevitably leads to a decrease in proton conductivity and an increase in cell resistance.

5.3.2 Non-covalent modified composite membranes. The methods for the preparation of non-covalent-modified membranes include blending, layer-by-layer self-assembly, and coating. Due to the absence of covalent bonds between the additives and the Nafion matrix, the water absorption and expansion behavior of the Nafion membrane will intensify the permeation of the vanadium ions in the composite membrane, leading to the degradation of battery performance. Therefore, it is crucial to obtain a uniform and stable composite membrane.

To suppress the water absorption and swelling of Nafion membranes, they can be blended with some hydrophobic components. There is a strong dipole–dipole interaction between the polar carbon fluorine bond of polyvinylidene fluoride (PVDF) and the carbonyl group of ester-containing polymers, which promotes the miscibility of PVDF with other polar polymers.[102,103] Mai *et al.* first blended PVDF with Nafion to prepare ion exchange membranes for VRFB. The addition of PVDF with high crystallinity and hydrophobicity effectively limited the swelling behavior of the Nafion membranes.[29] The VRFB assembled with PVDF/Nafion membrane exhibited a higher coulombic efficiency at different current densities and had a longer open circuit voltage retention time (80 h) compared to the battery with the original Nafion membrane. Similarly, Teng *et al.* blended hydrophobic polytetrafluoroethylene (PTFE) with Nafion to prepared a Nafion/PTFE composite membrane *via* the solution casting method,[104,105] which improved the crystallinity and thermal stability of the Nafion membrane and decreased the permeability of vanadium ions. However, although the above-mentioned polar polymers have high miscibility with Nafion, their hydrophobicity also reduces the ion exchange capacity and conductivity of the composite membrane.

As shown in Fig. 9b, another commonly used method for non-covalent modification is layer-by-layer self-assembly. Lu *et al.*[50] prepared Nafion-[CS-PWA]$_n$ by the self-assembly of cationic chitosan (CS) and negatively charged phosphotungstic acid (PWA). The Nafion-[CS-PWA]$_n$ membrane exhibited much lower vanadium ion permeability and the battery with this membrane showed a higher coulombic efficiency and energy efficiency, and slower self-discharge rate in comparison to that with Nafion 212. J. grosse Austing *et al.* also obtained an N117-(PEI/Nafion)$_k$ composite membrane using the same method and this membrane was used in a vanadium/air redox flow battery.[106] However, the process of self-assembly is based on the electrostatic interaction between different layers with opposite charges. Therefore, delamination or detachment of the multilayer composite membranes may occur during the operation of VRFB, leading to the degradation of battery performance.

In recent years, several organic materials for the modification of Nafion membranes have emerged, which are usually immiscible with the membrane substrate, thus exhibiting good dispersion and chemical stability. Yang *et al.* found that PWA is beneficial for proton transport, while nano Kevlar fibers (NKF) inhibited the permeation of vanadium ions.[107] Therefore, NKF were immobilized on PWA by hydrogen bonding, and then NKF@PWA was dispersed in a Nafion matrix to prepare a Nafion-(NKF@PWA) composite membrane *via* the solution casting method. Yang also coupled PWA with ammonified UiO-66 to prepare a Nafion-(UiO-66-NH$_2$@PWA) composite membrane.[108] In addition, Ye *et al.* utilized lignin, a natural polymer rich in hydroxyl groups with excellent dispersibility, to prepare a Nafion/lignin composite membrane through simple solution casting, and the assembled batteries could stably cycle 1000 times.[109] Lee *et al.* doped organic sulfonated copper phthalocyanine in Nafion to improve its resistance to vanadium ions.[110]

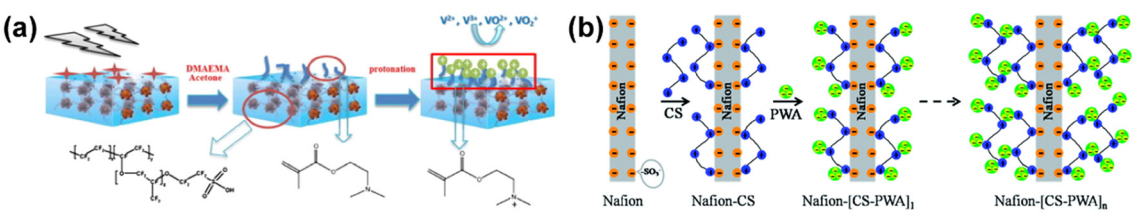

Fig. 9 (a) Preparation of radiation-induced grafted Nafion-*g*-PDMAEMA and protonated Nafion-*g*-PDMAEMA. Reproduced from ref. 100 with permission from Elsevier, Copyright 2013. (b) Schematic diagram of layer-by-layer self-assembly of Nafion-[CS-PWA]$_n$ membrane. Reproduced from ref. 50 with permission from The Royal Society of Chemistry, Copyright 2014.

As mentioned above, in recent years, there have been many studies on the modification of Nafion membranes aimed at improving their performance. The research results are summarized in Table 2. It cannot be ignored that the high cost of Nafion greatly limits the large-scale application of flow batteries, and thus the development of CEM without Nafion has become a research hotspot in recent years.

6. Other cation exchange membranes

6.1 Polytetrafluoroethylene (PTFE)-based CEM

The perfluorocarbon structure of PTFE ensures the high chemical and mechanical strength of membranes, but PTFE membranes have low proton conductivity due to the lack of ion exchange groups. Therefore, previous studies aimed to introduce components with high proton conductivity in the PTFE matrix to improve its proton conductivity.

Teng *et al.* used a solution impregnation method, in which a PTFE membrane was first impregnated with Nafion to prepare a PTFE/Nafion (P/N) composite membrane, and then the P/N membrane was further impregnated in tetraethoxysilane (TEOS) solution to fabricate the PTFE/Nafion/SiO_2 (P/N/S) composite membrane.[56,111] Ye *et al.* proposed a solution casting method by first dispersing functionalized silicon carbide nanowires (f-SiC) or acid-etched graphene oxide (d-GO) nanosheets in a perfluorosulfonic acid (PFSA) matrix, and then coating them on both sides of an ultra-thin PTFE layer to prepare a composite membrane.[43,112] As shown in Fig. 10a and b, the uniformly dispersed d-GO nanosheets or f-SiC nanowires provide more pathways for proton transport, and thus enhance the proton conductivity of the membrane (14.3 mS cm^{-1} for d-GO@PFSA-PTFE composite membrane). The PTFE layer as the core layer can effectively suppress the expansion rate and improve the stability of the membrane. As shown in Fig. 10c and d, the battery assembled with the PTFE@PFSA/f-SiC membrane had a lower self-discharge rate (with an open circuit voltage holding time of 113.1 h), endowing the battery with a higher efficiency and cycle stability in 1000 cycles. In addition, Teng *et al.* used a layer-by-layer self-assembly method to prepared ultra-thin (~30 μm) polycation poly(diallyl dimethylammonium chloride) (PDDA)/polyanion poly(sodium styrene sulfonate) (PSS) (named as P/S) films on PTFE.[113] The membrane showed good ion selectivity and the VRFB with the P/S-$(PDDA/PSS)_6$ membrane exhibited improved cycling stability.

6.2 Sulfonated polyetheretherketone (SPEEK)-based CEM

SPEEK is a polymer obtained by sulfonating polyetheretherketone (PEEK), and thus SPEEK membranes usually exhibit sufficient proton conductivity. In addition, they are easy to prepare and cost-effective, and present lower permeability to vanadium ions. However, SPEEK exhibits high swelling, poor mechanical stability and high vanadium ion crossover when the polymer matrix is highly sulfonated.[114,115]

Previous reports have shown that the addition of inorganic nanoparticles, such as WO_3,[116] and TiO_2,[117,118] is a feasible way to limit the swelling of SPEEK and reduce the permeability of vanadium ions due to the formation of hydrogen bonds. Wang *et al.* demonstrated that doping of hydrophilic TiO_2 nanoparticles in a SPEEK membrane could improve its proton conductivity (14.3 mS cm^{-1}).[119] Myures *et al.* also prepared a hydroxy boron nitride (OH-BN)-reinforced SPEEK composite membrane using a simple phase conversion technique.[120]

Carbon materials are also good candidates for the modification of SPEEK by doping. Luo *et al.* used functionalized carbon black (FCB) particles as fillers to obtain advanced SPEEK/FCB composite membranes.[45] As shown in Fig. 11a–c, the SPEEK/FCB-3 composite membrane exhibited excellent ionic selectivity (~1.2×10^6 S min cm^{-3}), low vanadium permeability and high proton conductivity compared to the original SPEEK and commercial Nafion 212 membrane. Moreover, Dai *et al.* prepared SPEEK/GO composite membranes using the conventional solution casting method.[121] As shown in Fig. 11d, the randomly embedded GO nanosheets in the SPEEK/GO membrane could act as an effective barrier to block the migration of vanadium ions, and significantly reduce their permeability. Zheng *et al.* used the same method to prepare a SPEEK/SGO composite membrane with sulfonated graphene oxide (SGO) nanosheets as a filler.[122] The layered structure of SGO and Donnan repulsion effect successfully suppressed the permeability of vanadium ions and exhibited high proton conductivity. Jia *et al.* and Ding *et al.* contributed to the uniform distribution of functionalized carbon nanotubes in the SPEEK matrix.[123,124] However, despite the significant advances, the durability of these composite membranes with carbon materials has not been fully examined in VRFB systems.

To improve the chemical stability and tensile strength of SPEEK, a polymer coating layer has been commonly used to reinforce the membrane. Zhao *et al.* used PVDF with high mechanical properties and good chemical stability to modify the surface layer of SPEEK.[126] The ion selectivity of the SPEEK/PVDF composite membrane was significantly improved and the VRFB with this membrane showed an enhanced performance. Xi *et al.* obtained a SPEEK/PDA composite membrane *via* the self-polymerization of a polydopamine (PDA) layer on the surface of SPEEK.[127] The PDA film acted as a barrier layer to protect the SPEEK membrane from corrosion by the high-oxidizing vanadium electrolyte. Recent research also utilized the reinforcing effect of PTFE to inhibit the water absorption and swelling ratio of SPEEK. In addition, the chemical and mechanical stability of PTFE can greatly improve the performance of the membrane. Wei *et al.* prepared PTFE-reinforced SPEEK composite membranes (SPEEK/PTFE)[128] and Yu *et al.* also demonstrated a PTFE/SPEEK/PTFE sandwich structure.[125] The VRFB based on this membrane exhibited an ultra-long lifespan (620 cycles), as shown in Fig. 11e.

In summary, most of the results based on SPEEK are listed in Table 2. However, due to its poor cycling stability and limited energy efficiency, especially at high operating current

Table 2 Preparation approaches, properties, and cell performance of modified membranes for VRFB

Membrane name	Preparation approach	Membrane properties							Mechanical properties	Cell performances							
		Thickness (μm)	Proton conductivity (mS cm^{-1})	Swelling ratio (%)	Water uptake (%)	Permeability of VO^{2+} ($\times 10^{-7}$ cm^2 min^{-1})	Ionic selectivity ($\times 10^5$ S min cm^{-3})	IEC (mmol g^{-1})	Tensile strength (MPa)	CE (%)	VE (%)	EE (%)	Current density (mA cm^{-2})	Capacity retention (%)	Cycle numbers	OCV holding time (h)	Ref.
Nafion/TiO_2	Sol–gel reaction	225	—	—	22.5	4.3	—	0.95	—	94.8	82.2	77.9	30	—	100	65	88
Nafion/SiO_2	Sol–gel reaction	204	56.2	—	21.5	—	—	0.96	—	86.7	92.1	79.9	20	—	100	35	90
Nafion/TiO_2 nanotube	Solution casting	36	—	—	—	—	—	—	26.54	98.3	83.0	84.4	120	55.7	1400	57.5	73
Nafion/$TiZrO_4$	Solution casting	—	75.9	—	—	0.21	36.1	—	—	99.8	84.1	83.9	80	74.7	300	382	96
Nafion/GO	Spin coating	57.4	0.41	9.6	13.1	0.82	—		21	95.0	84.2	80.0	80	—	200	—	55
CLGO/Nafion212	Spin coating	—	—	11.5	17.1	3	—	0.89	18.5	96.9	86.0	83.3	100	55.0	180	—	98
Nafion-(NKFs@PWA)	Solution casting	—	61	—	—	2.46	2.48	0.952	35.2	87.0	92.0	80.2	40	82.55	100	76	107
Nafion-(UiO-66-NH_2@PWA)	Solution casting	—	92	—	25.1	3.46	2.66	0.964	31.3	86.4	94.0	81.2	100	—	—	56	108
Nafion/lignin	Solution casting	~39	15.7	—	4.5	0.85	—	—	—	97.4	84.9	82.7	120	52.8	1000	87	109
PTFE@PFSA/f-SiC	Solution casting	37	—	—	—	0.67	2.31	—	27.23	96.2	90.5	87.1	120	—	—	113.1	43
d-GO@PFSA-PTFE	Solution casting	—	14.3	—	—	2.78	0.73	—	24.4	97.0	89.6	86.9	120	—	400	—	112
SPEEK/G-AMH-3	Solution casting	—	19.7	12	30.2	9.6	0.25	1.65	34.3	~91	—	~88	40	84.7	100	—	115
SPEEK/$(WO_3)_{0.20}$	Solution casting	—	—	—	30.2	—	0.21	1.52	—	~95	~88	~84	20	—	—	60	116
SPEEK/TiO_2	Solution casting	82	18.3	—	—	0.18	1.02	—	—	99.3	85.4	84.8	120	86.8	200	87.5	117
SPEEK/s-TiO_2	Solution casting	93	61	—	30.1	8.55	0.713	1.59	—	95.3	84.9	82.3	50	86.9	20	—	119
SPEEK/0.05 OH-BN	Phase inversion	135	26.4	17.5	36.8	—	0.53	—	—	94.2	87.2	82.12	40	—	—	14.21	120
SPEEK/FCB-3	Solution casting	62	—	9.84	18.52	—	—	1.24	—	99.5	83.9	83.5	120	44.64	1062	350	45
SPEEK/SGO-3	Solution casting	—	17.6	9.1	34.7	—	0.26	1.86	—	95.6	84.8	81.1	30	—	—	~52	122
SPEEK/MWCNTs-OH	Solution casting	—	—	—	—	1.93	—	—	61.8	99		80	50	73	500	100	124
SPEEK/PVDF ($S_{0.7}/P_{0.3}$)	Solution casting	200	70.0	—	24.5	1.60	4.4	1.59	42.3	97.4	85.4	83.2	30	—	100	150	126
SPEEK/PTFE	Solution casting	—	—	—	—	—	—	—	39.47	93.4	89.6	83.7	80	—	700	~28	128
SPI/TiO_2	Solution casting	49	31.2	12.5	32.94	2.02	1.54	1.243	—	~97	~72	~70	70	—	—	~165	129
SPI/s-MoS_2	Solution casting	66	27.5	16.18	23.2	1.23	2.24	1.698	—	~100	~72	~72	70	—	500	193	132
bSPI/s-MWCNTs-1%	Solution casting	47	—	14.7	36.5	2.01	1.06	1.23	28.4	96	83	79.7	80	—	400	44	133
PVA/OMS-7	Solution casting	—	69.14	—	27.5	0.135	—	0.695	—	97.3	83.8	81.51	30	—	100	~71	139
SPI5/PVA5	Solution casting	84	31.7	27.3	35.2	11.3	—	0.65	—	96.3	82.6	79.5	30		100	68	140
SPI-B-50	Solution casting	40	16.4	10.0	24.3	0.71	2.31	1.25	38.26	97.5	—	~92	80	68.3	100	44	138
6F-s-bSPI	Solution casting	35	20.6	19.0	25.7	1.18	1.75	1.54	78.3	~99	~77	~76	60	69.8	100	—	141
TM-OPBI-12	Solution casting	—	13.3	13.8	22.1	—	—	—	—	~100	~67	68.2	160	93.9	500	263	145
B-PBI	Solution casting	33	—	—	—	1.59	—	—	—	99.2	84.1	84.8	80	—	200	—	146
P-20-7	Electrostatic spinning	—	57.0	4.4	200.2	7.30	—	—	36.2	~99	~84	82.0	150	62.0	200	—	148
SPPEK-P90	Solution casting	53	—	15.6	23.2	—	—	1.51	71	98.2	88.8	87.2	40	—	100	290	151
SPES/S-ZrO_2-10	Solution casting	55	—	9.2	36.2	~0.3	—	1.31	—	98.9	87.8	86.8	100	—	70	63	154
HSPAEK	Solution casting	60	33.4	11.6	38.5	5.50	0.367	1.72	27.4	99.0	84.8	84.0	80	83.0	100	202	156
QPAPEKK-110	Solution casting	40	—	~10	—	8.57	—	0.62	33	~91	~89	86.7	160	~61	1000	—	159
PFDP-90	Solution casting	42	—	5.9	—	0.10	—	~2.7	45.2	~96	~88	83.1	120	—	1000	~30	160
PS-DTQG-5	Solution casting	12.5	60.6	18.0	32.5	0.32	0.36	2.14		98.1	78.0	76.4	60	—	80	120.8	161
PSf-MIm-1.2	Solution casting	—	22.6	19.8	67.5	18.12	—	1.53	10.8	97.0	84.9	82.4	120	—	4800	—	162
PBI-21%EPTMA	Solution casting	47	—	—	—	5.11	—	—	56	~99	~81	81.0	100	—	450	—	163
HPSf-Im-CD30%	Solution casting	61	100.0	7.5	25.5	0.92	10.82	0.76	—	~97	~82	80.0	120	—	50	73	168
BVSN-porous-3	Solution casting	—	77.0	13.2	30.2	0.78	9.9	2.31	—	97.3	85.0	82.7	80	—	100	300	169
PE/PP-*g*-PVBTMA (210%)	Phase inversion	21	39.4	38.0	93.6	2.3	—	3.6	22.6	~93	—	~82	80	—	100	50	170
ETFE-*g*-PSSA	Radiation grafting	38	24.0	—	14.7	0.39	—	0.88	—	~95	~78	~72	40	—	40	300	177
C-SPEEK-50	Solution casting	—	—	—	—	—	—	1.34	—	98.0	87.0	85.3	80	—	180	—	178
SPI/0.5% PDAP	Solution casting	60	133.0	28.0	38.5	0.14	1.55	1.49	—	96.6	87.0	84.0	100	—	500	—	180
PFSPI-PAA-25	Solution casting	—	30.7	18.7	37.2	0.06	—	1.53	—	98.0	86.7	85.0	140	—	500	52.3	137
SPI/PEI-rGO-2	Solution casting	—	~4.8	7.1	44.2	—	0.09	1.16	52.6	95.0	79.6	75.6	40	—	100	~80	181
bSPI-8	Solution casting	60	4.4	23.2	40.2	6.27	0.7	1.40	72.94	97.0	82.5	80.0	50	—	800	180	182
TA15-SPBP	Solution casting	—	116.0	11.0	38.0	0.79	14.7	1.98	44.3	99.1	87.8	87.0	80	80.5	200	—	187

Table 2 (Contd.)

Membrane name	Preparation approach	Membrane properties							Mechanical properties	Cell performances						Ref.
		Thickness (μm)	Proton conductivity (mS cm^{-1})	Swelling ratio (%)	Water uptake (%)	Permeability of VO^{2+} ($\times 10^{-7}$ cm^2 min^{-1})	Ionic selectivity ($\times 10^5$ S min cm^{-3})	IEC (mmol g^{-1})	Tensile strength (MPa)	CE (%)	VE (%)	EE (%)	Current density (mA cm^{-2})	Capacity retention (%)	Cycle numbers	OCV holding time (h)	
PBI-OSO_3^-/OHN^+-0.47	Solution casting	—	—	—	—	0.02	58.9	0.47	—	99.2	86.6	85.9	100	69.0	100	—	184
PVDF/SiO_2–SO_3H-42	Phase inversion	—	14.0	0.5	52.1	1.12	1.25	—	—	90.3	83.7	75.6	60	—	30	~32	195
M90	Phase inversion	130	—	—	—	—	—	—	—	90.3	86.8	78.4	80	—	300	—	196
TMA-5	Phase inversion	45	—	6.8	—	—	—	4.41	—	~99	~90	~88.5	80	—	1500	100	201
PPY/PES	Phase inversion	—	—	—	—	0.07	—	—	—	87.3	91.9	80.2	80	—	100	—	202
PS-IPA	Phase inversion	—	—	—	—	—	—	—	—	98.5	91.8	90.4	80	—	500	—	205
PES/SPEEK-M3	Solvent-template	65	—	—	—	—	—	—	—	99.0	92.9	92.0	40	—	100	—	206
PES (10% P)	Phase inversion	—	—	—	—	0.14	—	—	—	94.5	86.4	81.7	80	—	70	—	207
P-5	Solution casting	30	—	—	—	8.24	—	—	—	95.2	92.2	87.8	80	—	200	—	208

densities, the wider application of SPEEK based membranes is still hindered.

6.3 Sulfonated polyimide (SPI)-based CEM

SPI, as a low-cost fluorine-free aromatic polymer, has been utilized in VRFB because of its good mechanical and chemical properties.

The introduction of inorganic additives can improve the performance of SPI membranes and the main additives include TiO_2,[129] ZrO_2,[130] AlOOH,[131] s-MoS_2 [132] and s-MWCNTs.[133] Among them, Li *et al.* prepared a composite membrane of SPI and sulfonated molybdenum disulfide (s-MoS_2) using a blending method.[132] Due to the enhanced hydrogen bonding between SPI and s-MoS_2, as well as the barrier effect of s-MoS_2 sheets, which were uniformly distributed along the cross-section of the membrane (Fig. 12a and b), the SPI/s-MoS_2 membrane was found to enable high proton conductivity (27.5 mS cm^{-1}), lower vanadium ion permeability (1.21×10^{-7} cm^2 min^{-1}) and good stability (500 cycles). Also, the self-discharge time of the cell was longer than that with a Nafion membrane (Fig. 12c).

In addition, the modification of SPI with polymers has been achieved by the immersion and self-assembly method. CS/SPI composite membranes have been proved to be effective in blocking vanadium ion permeation.[134–136] The cross-linking structure of CS and the blockage of micropores by CS in CS/SPI composite membranes significantly inhibit the crossing of vanadium ions. Li *et al.* synthesized a sulfonated polyimide polymer (PFSPI) with polyurea structure, and further modified PFSPI with polyacrylic acid (PAA) to prepare a novel PFSPI-PAA-X composite membrane.[137] This membrane exhibited low area resistance and low vanadium permeability. The assembled VRFB showed a lower self-discharge rate (with an open circuit voltage holding time of 52.3 h), demonstrating excellent durability in 500 cycles.

To enhance the proton conductivity of SPI, hydrophilic polyvinyl alcohol (PVA) can be blended with SPI to form a microstructure with highly dispersed phase separation, which keeps the hydrophobic main chain away from water molecules, thereby improving the chemical stability and proton conductivity of SPI.[139,140] It is worth noting that using the branching structure of SPI to prepare composite membranes can also improve the limitation of poor microphase separation in pure SPI. Li *et al.* developed a branched SPI-B membrane[138] and 6F-s-bSPI membrane[141] *via* the high-temperature condensation method. As shown in Fig. 12d, the branched sulfonated polyimide (SPI-B) membrane, consisting of 2-methyl-1,4-bis(4-amino-2-trifluoromethyl) benzene (FAPOB) as a functional diamine monomer, exhibited an excellent vanadium ion blocking performance and proton conductivity. The SPI-B membrane with a sulfonation degree of 50% (SPI-B-50) exhibited a higher coulombic efficiency, voltage efficiency and energy efficiency, and longer lifespan in VRFB compared to that with Nafion (Fig. 12e and f).

In summary, although modified SPI membranes result in an improved battery performance compared to the original SPI

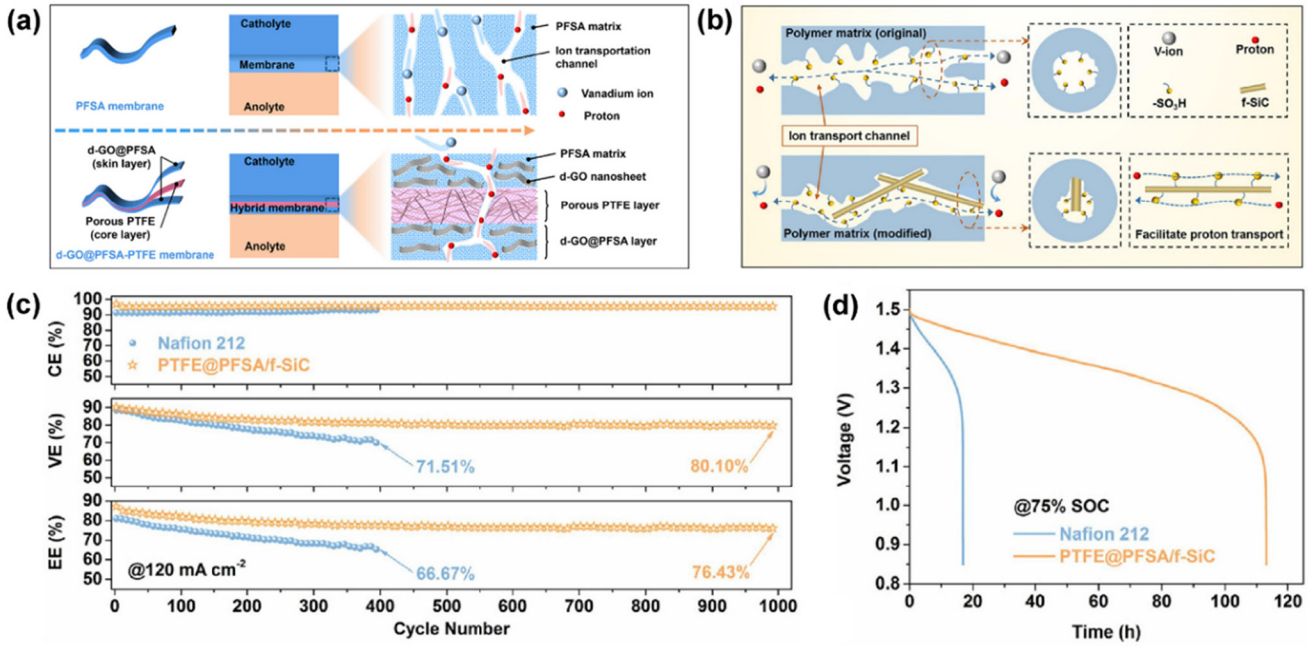

Fig. 10 Schematic illustration of the permeation of vanadium ions and proton transportation. (a) VRFB assembled with d-GO@PFSA-PTFE. Reproduced from ref. 112 with permission from Elsevier, Copyright 2022. (b) VRFB assembled with PTFE@PFSA/f-SiC. (c) Coulombic efficiency, voltage efficiency and energy efficiency and (d) open circuit voltage attenuation curves of VRFB assembled with Nafion 212 and PTFE@PFSA/f-SiC membranes. Reproduced from ref. 43 with permission from Elsevier, Copyright 2021.

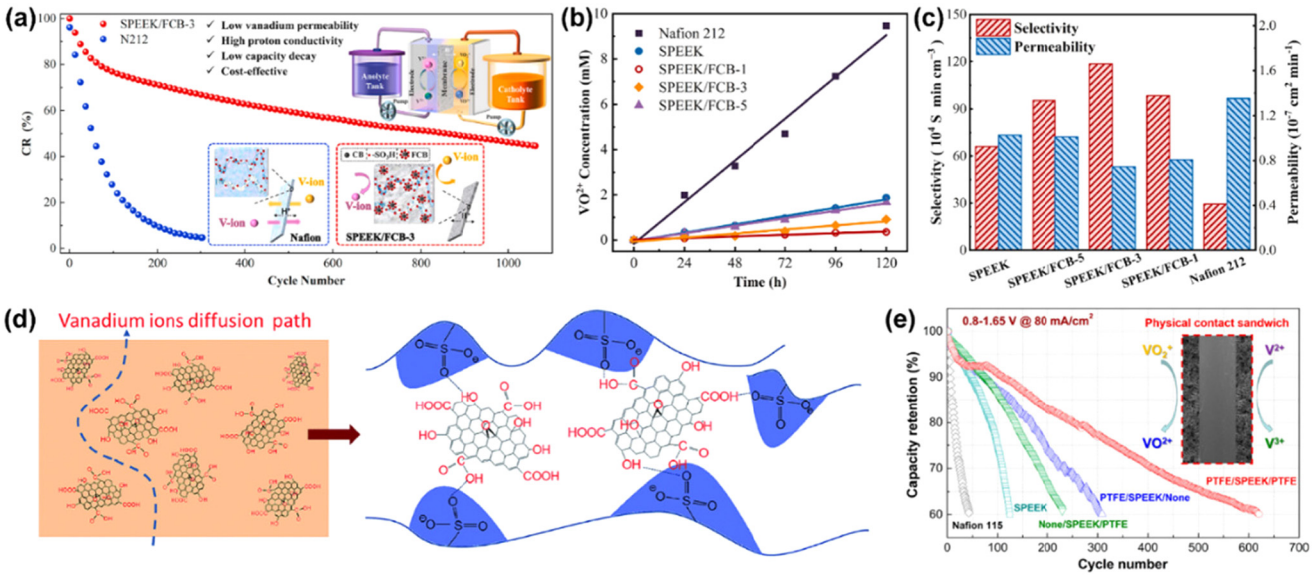

Fig. 11 (a) Schematic of SPEEK/FCB composite membrane in a VRFB cell. Measurement of (b) concentration as a function of time and (c) permeability and ion selectivity of vanadium ions with different membranes. Reproduced from ref. 45 with permission from Elsevier, Copyright 2021. (d) Mechanism of vanadium ion migration in S/GO composite membrane. Reproduced from ref. 121 with permission from The Royal Society of Chemistry, Copyright 2014. (e) Cycling performance of VRFB assembled using various membranes. Reproduced from ref. 125 with permission from the American Chemical Society, Copyright 2016.

membrane, as shown in Table 2, their proton conductivity remains at a relatively low level throughout the ion exchange membrane, thus further efforts should be devoted to further optimizing the structural regulation/recombination.

6.4 Polybenzimidazole (PBI)-based CEM

PBI has a highly stable polymer framework and low cost, making it a promising membrane material for application in

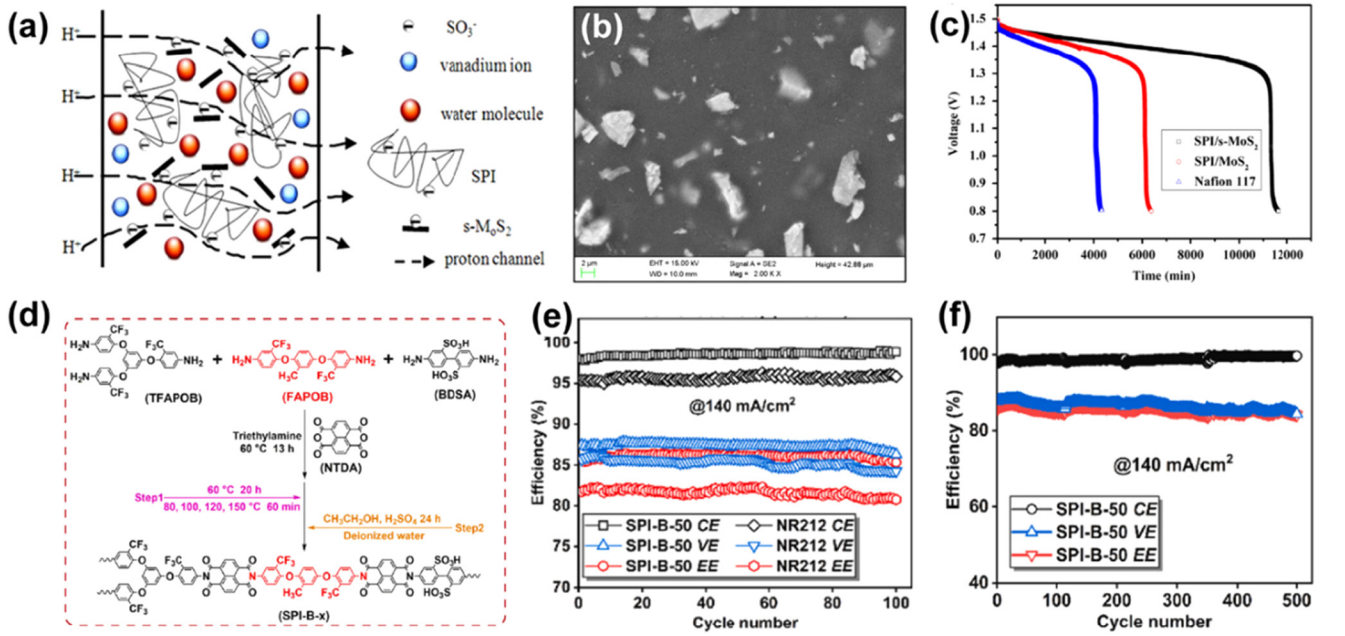

Fig. 12 (a) Proton transport mechanism and (b) surface morphology of SPI/s-MoS_2 composite membrane. (c) Open circuit voltage of VRFB with SPI/s-MoS_2, SPI/MoS_2 and Nafion 117 membranes. Reproduced from ref. 132 with permission from Elsevier, Copyright 2015. (d) Synthetic pathway of SPI-B membranes. (e) Performances of VRFB with SPI-B-50 and NR212 membranes during 100 cycles. (f) Performance of VRFB with SPI-B-50 membrane during 500 cycles. Reproduced from ref. 138 with permission from Elsevier, Copyright 2023.

acidic and oxidizing conditions. The results show that the pore size of PBI films is about 0.5–2.0 nm, which is helpful to reduce the crossover of vanadium ions through the membrane.[142,143] However, the proton conductivity of pure PBI membranes is very low (~10^{-12} S cm^{-1}),[144] and acid-doping and protonating N atoms in PBI are needed to improve the proton mobility.

The dense skeletal structure of PBI and the strong hydrogen bonding between the main chains are insensitive to the general method of acid doping such as soaking pretreatment. Therefore, adding side chains and copolymerization modification are usually adopted to endow PBI with a larger free volume for higher degree of acid doping. For example, Ding *et al.* synthesized a PBI membrane with thiophene ring side group (TM-OPBI)[145] and the presence of thiophene side groups enlarged the free volume of the membranes. The alkaline heterocycle could improve the proton conductivity of the membrane, and the positively charged thiophene side could enhance the vanadium resistance performance through the Donnan effect. In addition, the VRFB assembled by the TM-OPBI membrane showed a capacity retention rate of 93.85% after 500 cycles at the current density of 160 mA cm^{-2}. In addition, Chen *et al.* introduced pyridine side chains and constructed a dual-channel PBI composite membrane with enhanced proton conductivity and vanadium ion selectivity.[146]

In addition, the thickness of PBI membranes has a great influence on their degree of acid doping degree and performance.[147] For instance, the voltage efficiency of the battery will increase with a thinner membrane thickness due to the lower ohmic resistance, and a battery with a thick PBI membrane will require a higher charge potential. This extra charge potential promotes the occurrence of side reactions and the permeation of vanadium ions through the membrane.[147] Although thinner PBI membranes can result in improved battery properties by acid doping, their mechanical stability and durability strength will be insufficient. Wan *et al.* prepared a double-layer PBI composite membrane (P-20-7),[148] which consisted of a dense and thin PBI underlayer (7 μm) as well as a porous and thick PBI surface layer, as shown in Fig. 13a and b. The dense layer served as a selective layer to ensure high ion selectivity, while the porous layer served as a support layer to guarantee mechanical stability. The energy efficiency of the cell with the P-20-7 composite membrane was nearly 20% higher than that with the traditional PBI film (Fig. 13c and d) and the cell also showed stable operation for 200 cycles with a capacity retention rate of 99.81%.

Besides the above-mentioned materials, polymers including sulfonated poly(phthalazinone ether ketone) (SPPEK),[149–151] sulfonated poly(ether sulfone) (SPES)[152–155] and sulfonated poly(fluorenyl ether ketone sulfone) (SPAEK)[156] have been explored to prepare CEMs for VRFB. However, there is no modified CEM that can completely replace or compete with commercial Nafion membranes. In the future, it is essential to develop more suitable membranes and simplify the production methods for achieving enhanced battery performances and low cost.

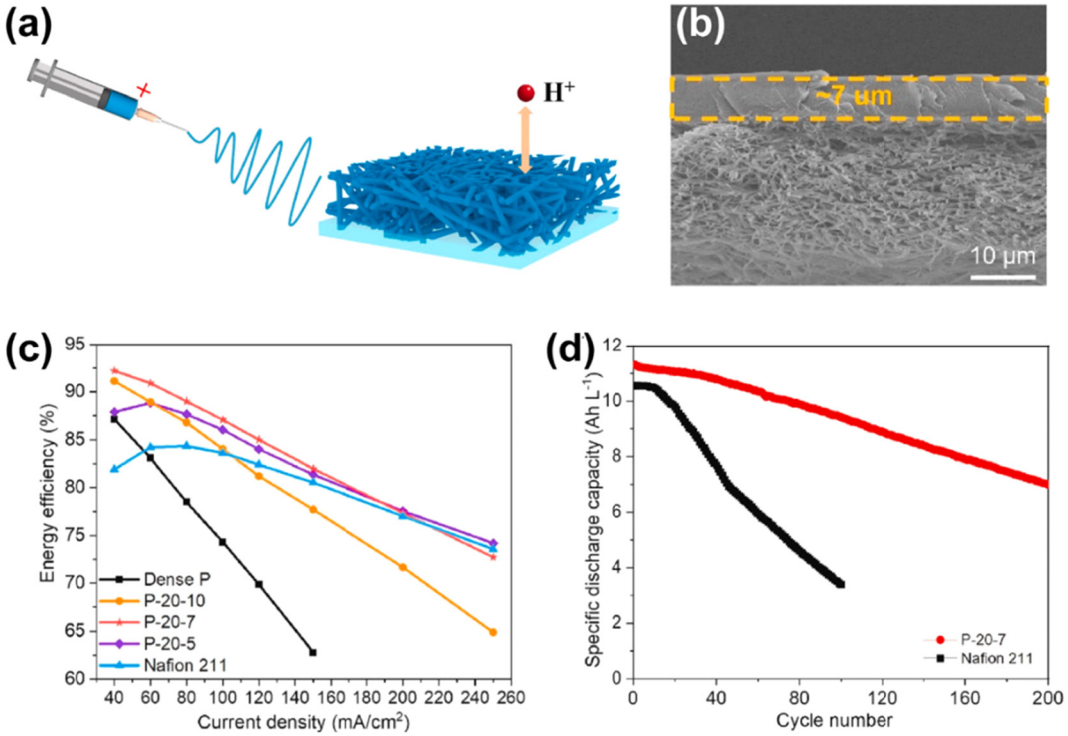

Fig. 13 (a) Illustrative scheme of PBI composite membrane supported by electrospun nanofibers. (b) SEM images of the cross-section morphology of P-20-7. (c) Energy efficiency of flow batteries assembled with PBI-based membranes and Nafion 211. (d) Specific discharge capacity of flow batteries assembled with P-20-7 membrane and Nafion 211 at a current density of 80 mA cm^{-2}. Reproduced from ref. 148 with permission from Elsevier, Copyright 2021.

7. Anion exchange membranes (AEMs)

AEMs are another type of polymer electrolyte membrane, in which cationic groups are immobilized on the polymer backbone, and thus they fundamentally prevent the crossover of vanadium species through the Donnan effect, exhibiting excellent ion selectivity. However, the stability of the functional cationic groups in AEMs is lower compared to that in CEMs, and then the degradation of the membrane leads to a shortened lifespan of VRFB. Furthermore, batteries with AEMs may have a low voltage efficiency due to the unfavorable effect on proton conduction in membrane. There has been a significant amount of research on improving the performance of AEMs, and some representative research results will be discussed in detail next.

7.1 Modification with inorganic additives

The early attempt of AEM modification involved adding inorganic additives of different densities to pure AEM. Li *et al.* prepared a composite AEM based on quaternary ammonium poly(aryl ether sulfone)/nano-zirconia (QPAES/ZrO_2) *via* the solution casting method, and applied it in a fuel flow cell.[157] The introduction of nano-ZrO_2 inhibited the crystallization of the QPAES matrix, significantly improving the IEC of the composite membrane. Moreover, Leung *et al.* modified a commercial AEM (Fumatech GmbH) *via* the sol gel method and prepared an SiO_2-doped composite AEM.[158] The uniformly dispersed SiO_2 nanoparticles formed a physical barrier, which could effectively block the crossing of vanadium ions. The VRFB assembled with the composite membrane exhibited a coulombic efficiency of 92% and energy efficiency of 73% at a current density of 40 mA cm^{-2}. It is worth noting that further study is needed to enhance the long-term chemical stability and aging performance of AEMs modified by inorganic additives.

7.2 Design of molecular structure

Most AEMs contain quaternary ammonium or other amine functional groups, which can be replaced by other groups to improve the membrane performance through molecular structure design. Zhang *et al.* prepared quaternized poly(aryl ether ketone ketone) (PAPEKK) membranes containing phenyl and adamantane groups, and the membranes were further soaked in phosphoric acid at different temperatures (40 °C, 90 °C and 110 °C) to induce selective swelling in the membranes with ion channels (QPAPEKK).[159] The area resistance of the QPAPEKK-110 membrane was only 0.24 Ω cm^2, while the VRFB assembled with QPAPEKK-90 showed an impressive energy efficiency of 91.4% and 80.0% at current densities of 80 mA cm^{-2} and 220 mA cm^{-2}, respectively.

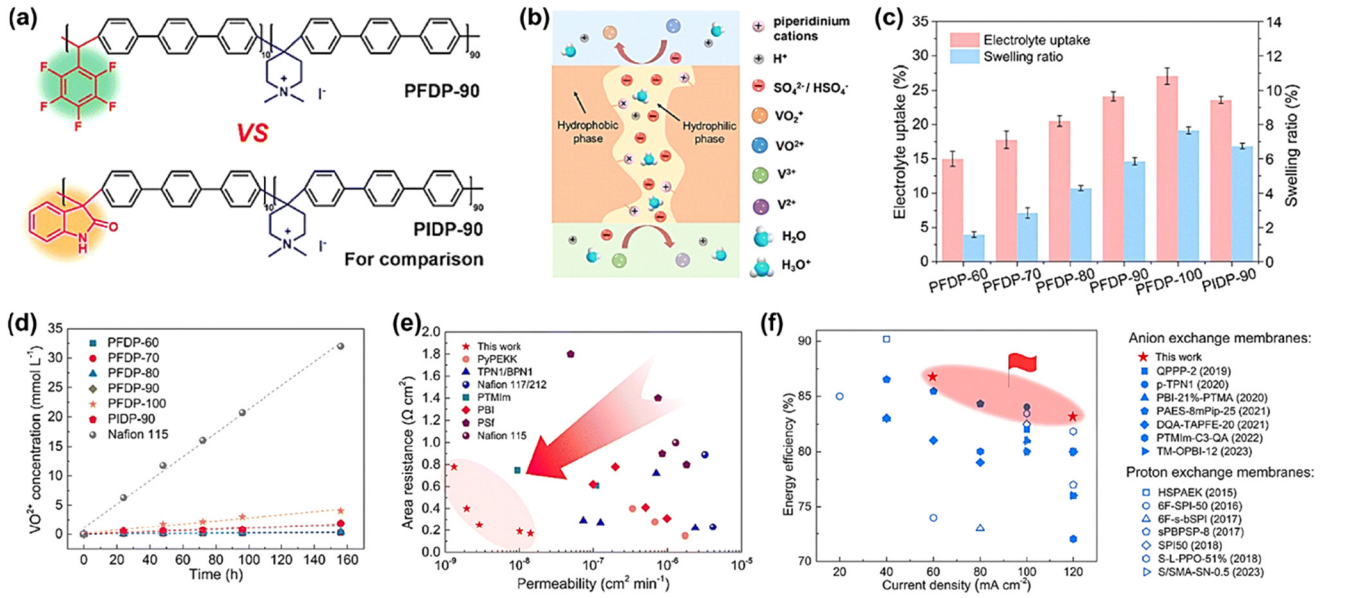

Fig. 14 (a) Comparison of the chemical structure of fluorinated and nonfluorinated poly(aryl piperidine) membranes. (b) Schematic diagram of interconnected hydrophilic channels with microphase separation. (c) Electrolyte uptake and linear swelling ratio of PFDP and PIDP membranes in 3 M H_2SO_4 solution at 30 °C. (d) Changes in VO^{2+} concentration on the permeation side of magnesium sulfate solution with time. (e) Comparison of area resistance and vanadium permeability of AEMs with different molecular designs and Nafion membranes. (f) Comparison of EE at different current densities between PFDP-90 and the reported unmodified polymer ion exchange membranes applied to VFBs. Reproduced from ref. 159 with permission from The Royal Society of Chemistry, Copyright 2023.

Ban *et al.* designed and synthesized a novel fluorinated poly (aryl piperidinium) (PFDP) anion exchange membrane.[160] As shown in Fig. 14a, the ether-free polymer skeleton and fluorinated structure of the PEDP membrane could synergistically improve the stability of the membrane. Meanwhile, the microphase separation channels were rich in quaternary ammonium groups, allowing the formation of continuous interconnected water clusters in the membrane, which achieved effective ion conduction, while effectively repelling vanadium ions (Fig. 14b). As shown in Fig. 14c–e, the prepared PFDP membrane exhibited low vanadium permeability ($<1.4 \times 10^{-8}$ cm^2 min^{-1}) and swelling ratio (<8%), high tensile strength (60 MPa) and chemical stability (>28 days in the antioxidant test). Due to these advantages, the cell assembled with PFDP-90 exhibited excellent energy efficiency (84.3%) at 120 mA cm^{-2} (Fig. 14f) and stable cycling for over 1000 cycles.

7.3 Design of microstructure

Besides the design of molecular structure, the microstructure of AEMs can be tailored by introducing other side groups into the main chain of the polymer. Shukla *et al.* connected quaternized GO (QG), which is grafted with a long alkyl chain (C16), with the polyethersulfone (PS) polymer backbone by 1,4-diazabicyclic[2,2,2]octane (DABCO) coupling, and obtained the PS-DTQG membrane with high performance.[161] The large number of amine groups in the PS-DTQG membrane improved the ionic conductivity, while its comb-shaped structure resulted in good hydrophilic/hydrophobic phase separation, which is beneficial for proton transport (60.6 mS cm^{-1}). Xing *et al.* transplanted imidazole groups in the main chain of polysulfone polymer (PSF) through an effective CuAAC click reaction, and the resulting membrane showed a very low area resistance.[162] The VRFB assembled with this membrane has a coulombic efficiency of 97.0% and an energy efficiency of 82.4%, and a long-term durability (4800 cycles) at a current density of 120 mA cm^{-2}.

Similarly, the composite AEMs prepared with PBI[163–165] and poly(arylene ether sulfone) (PAES)[166] as the main chain of the polymer also showed great application potential. For example, Ren *et al.* synthesized a series of quaternary ammonium-grafted PBI membranes (PBI-EPTMA) using 2,3-epoxypropyl trimethyl ammonium chloride (EPTMA-Cl) as the grafting agent.[163] Grafting EPTMA group increased the hydrophilicity and free volume of the membrane, which led to an increase in the amount of sulfuric acid doping and decrease in the area resistance. The VRFB assembled with PBI-21% EPTMA exhibited a higher energy efficiency (87.6%–75.3%) at current densities varying from 50–150 mA cm^{-2} compared to that with Nafion 115 (81.7%–61.2%), and good cycling stability for 450 cycles.

7.4 Control of preparation process

The microstructure of AEMs is also strongly related to their preparation method, and thus effective regulation of their preparation process is crucial for improving their performance.[167] For example, Ma *et al.* dispersed β-cyclodextrin (β-CD) into a hydroxyl modified polysulfone precursor (HPSf-Im) using the template method, and then removed the template to obtain AEMs with a fine pore structure.[168] The hydrogen bonding between β-CD and the polymer matrix was beneficial to reduce the agglomeration of β-CD, and then promote the

formation of a pore structure in the membrane. Owing to the synergistic effect of nanopores and imidazole cation, the prepared AEM exhibited a low IEC, high conductivity, and low vanadium ion permeability. The VRFB using this membrane showed a coulombic efficiency of 99% and energy efficiency of 80% at a current density of 120 mA cm^{-2}.

Moreover, Ma *et al.* prepared a nano-porous AEM *via* the hydrolysis crosslinking method.[169] The pores in the membrane provided an effective pathway for proton transport due to the Donnan repulsion effect, while quaternary ammonium functionalized crosslinking further inhibited membrane expansion and vanadium ion penetration. Therefore, the prepared membrane combined the advantages of ionic and porous membranes. The VRFB assembled with this membrane showed stable cycling for 100 times at a current density of 80 mA cm^{-2}, with a coulombic efficiency of 97.3% and energy efficiency of 82.7%.

Abdiani *et al.* prepared a PE/PP-*g*-PVBC membrane *via* the radiation graft copolymerization of polyvinyl chloride benzyl (PVBC) and polyethylene/polypropylene (PE/PP) microfibers, and further converted it into a dense membrane with quaternary amine groups.[170] This membrane exhibited high ionic conductivity, low vanadium permeability and good chemical and mechanical stability. The VRFB assembled with the PE/PP-*g*-PVBC membrane exhibited a much lower vanadium ion permeability and higher energy efficiency than that with a Nafion membrane at a current density of 80 mA cm^{-2}.

Although numerous studies have made efforts to improve the ion conductivity and stability of AEMs, the adverse effects of proton conduction lead to a low voltage efficiency in VRFB. In addition, further molecular structure and microstructure design are needed, and preparation methods need to be further optimized to improve their comprehensive performance.

8. Amphoteric ion exchange membranes (AIEMs)

CEMs have excellent chemical stability and superior ionic conductivity, but typically have high vanadium ion permeability. On the contrary, AEMs can significantly inhibit the crossing of vanadium ions (Donnan effect), but their low ion conductivity leads to greater capacity loss and low voltage efficiency. To obtain both high ionic conductivity and low vanadium ion crossing in the membrane, Sollner first proposed a membrane containing both cationic and anionic groups in 1932, and named it an amphoteric ion exchange membrane (AIEM).[171]

The selectivity of vanadium ions can be significantly improved by introducing positively charged groups or doping inorganic materials in CEMs such as Nafion membranes, which are attractive routes to prepare AIEMs. However, the application of Nafion-based membranes is always limited by their high cost. The preparation of Nafion-based membranes was discussed in previous sections. Here, the development of partially fluorinated or non-fluorinated membranes as AIEM will be review and the typical polymer materials are PVDF,[172–177] SPEEK,[178,179] SPI[180–182] and other materials.[69,183–190]

8.1 Poly(vinylidene fluoride) (PVDF)-based AIEM

The introduction of anionic functional groups in PVDF by the irradiation grafting process has been widely reported. As shown in Fig. 15a and b, Qiu *et al.* developed AIEM *via* one-step grafting (AIEM-I) and two-step modification (AIEM-II).[174,177] AIEM-II avoided the degradation of the quaternary ammonium groups caused by chlorosulfonic acid, showing high IEC, conductivity, and low vanadium ion permeability. Specifically, styrene (St) was first grafted to a poly (ethylene-*co*-tetrafluoroethylene) (ETFE) membrane, followed by sulfonation to obtain ETFE-*g*-PSSA, and then grafted with dimethylaminoethyl methacrylate (DMAEMA) and protonated to obtain AIEM-II. As shown in Fig. 15c, the open circuit voltage of VRFB assembled with AIEM-II could be maintained above 1.3 V after 300 cycles, and its coulombic efficiency and energy efficiency were higher than that with the Nafion membrane. As shown in Fig. 15d, Ma *et al.* also prepared an AIEM based on the radiation grafting of PVDF powder and solution phase inversion method.[176] The grafting ratio for powder irradiation grafting was higher than that for direct grafting on the membrane, and therefore the IEC of the AIEM is increased and its vanadium ion permeation was remarkably suppressed. However, the mechanical stability of AIEM will decrease if the grafting ratio is too high. In addition, the radiation source will be destructive to the polymer structure, which is unfavorable to the mechanical and chemical stability of AIEMs.

8.2 Sulfonated poly(ether ether ketone) (SPEEK) based AIEM

Chen and Li dissolved sulfonated poly(etheretherketone) (C-SPEEK) in dimethylacetamide, and then poured the solution on a glass plate and dried it at 70 °C for 12 h to obtain a film. The film was peeled and soaked in 0.5 M sulfuric acid for 24 h to fabricate a SPEEK membrane with suspended carboxylic acid groups.[178] The introduction of carboxylic acid groups could effectively improve the IEC of the C-SPEEK membrane. Compared with Nafion 115, the VRFB assembled with the C-SPEEK-50 membrane showed a higher energy efficiency (85% *vs.* 82%) and coulombic efficiency (97.3% *vs.* 94.6%). Also, it still had good stability after more than 180 cycles. Jung *et al.* also introduced a small amount of urethane acrylate non-ionomer (UAN) in a blend of SPEEK and PVDF and prepared a SPEEK/PVDF/UAN membrane *via* the solution casting method.[179] The blended membrane combined the advantages of high proton conductivity of SPEEK and low vanadium permeability of PVDF. Therefore, the VRFB assembled with the three-phase blended membrane showed a significant improvement in discharge capacity and energy efficiency compared to that with the SPEEK/PVDF membrane or Nafion 212 membrane.

8.3 Sulfonated polyimide (SPI)-based AIEMs

Zhang *et al.* prepared a blended membrane of SPI and poly[bis (4,4′diaminobenzidine-2,2′-disulfonic acid) phosphazene] (PDAP) *via* the solution casting method.[180] PDAP contains

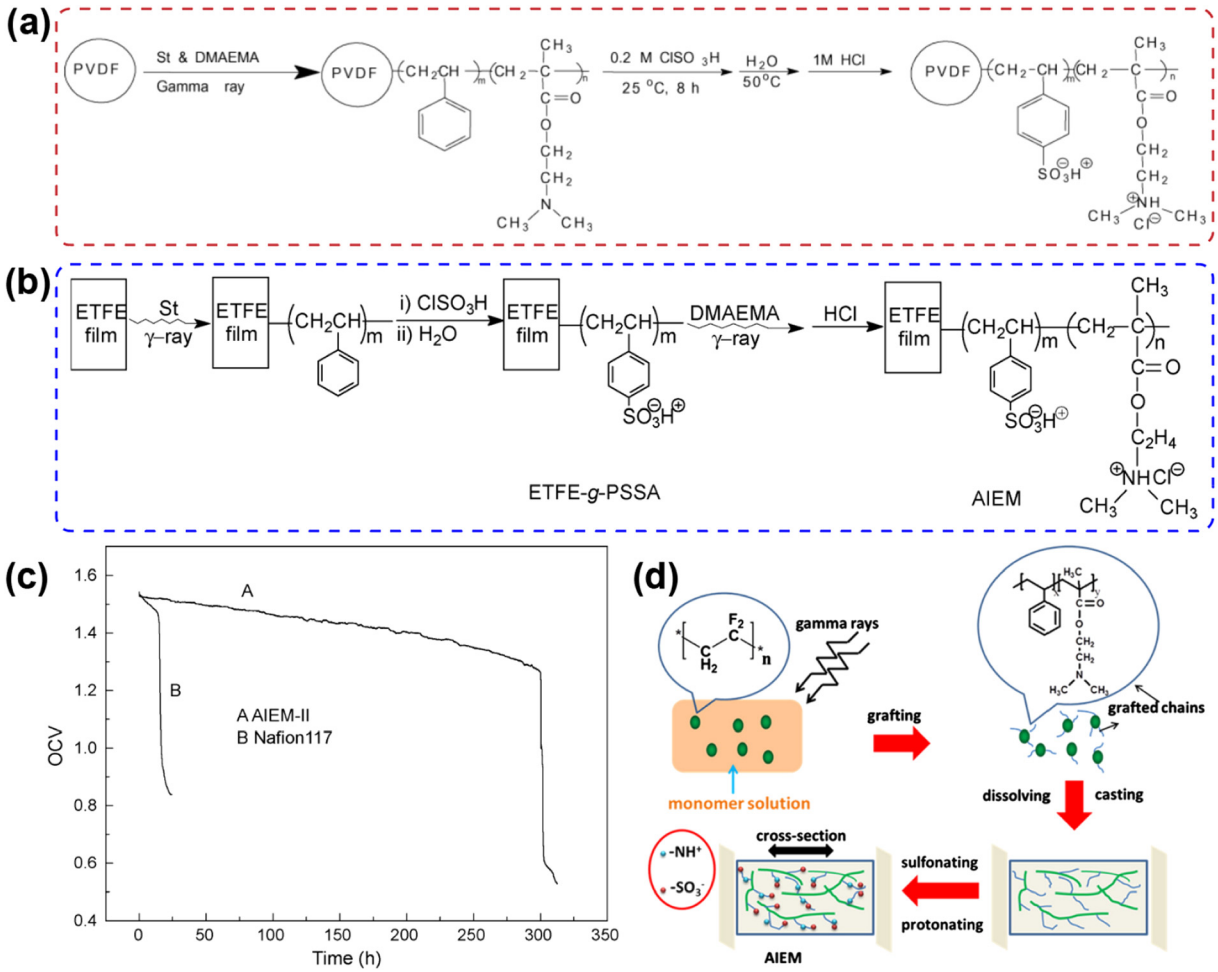

Fig. 15 (a) Preparation of AIEM-I *via* one-step modification. Reproduced from ref. 174 with permission from Elsevier, Copyright 2009. (b) Preparation of AIEM-II by two-step modification. (c) Open circuit voltage of VRFB with AIEM-II and Nafion 117 membranes. Reproduced from ref. 177 with permission from Elsevier, Copyright 2009. (d) Schematic diagram of AIEM prepared by radiation grafting method and solution phase inversion method. Reproduced from ref. 176 with permission from Elsevier, Copyright 2012.

amphoteric functional groups, which provide more groups ($-SO_3H$) for proton transport, and the protonated N atoms can block the permeation of vanadium ions by the Donnan repulsion effect. Therefore, the SPI/PDAP membranes exhibited high proton conductivity (up to 1.33×10^{-1} S cm^{-1} at room temperature) and low vanadium permeability (1.37×10^{-8} cm^2 s^{-1}). As shown in Fig. 16a–c, the coulombic efficiency and energy efficiency of the VRFB assembled using the SPI/PDAP membrane were higher than that with Nafion 212. Moreover, the battery could be continuously and stably cycled for 500 times at the current density of 100 mA cm^{-2}. Li *et al.* developed a new covalently cross-linked polyfluorinated sulfonated polyimide membrane (PFSPI-PAA-X) using hydrophilic PAA as a crosslinking agent.[137] As shown in Fig. 16d, the polymer structure containing C–F bond exhibited excellent chemical stability in the VRFB, and the hydrogen bond network formed by F element and H_2O could improve the proton conductivity of the membrane. In addition, the cross-linking of PAA and PFSPI promoted the proton transport and effectively limited the penetration of vanadium ions due to the hydrophilic/hydrophobic phase separation structure. As shown in Fig. 16e, the membrane exhibited very low vanadium permeability, which is two orders of magnitude lower than that of the Nafion 212 membrane. The VRFB assembled with the PFSPI-PAA-25 composite membrane maintained a high efficiency, peak power density, and excellent durability during 500 cycles (Fig. 16f–h). Similar studies on SPI-based AIEMs include a new acid–base hybrid membrane (SPI/PEI-rGO) synthesized by Cao *et al.*[181] and branched sulfonated polyimide (bSPI) membrane reported by Zhang *et al.*[182]

8.4 Other AIEMs

Xu *et al.* prepared sulfonated polybiphenyl tethered with pendant tertiary amine groups (TA-SPBP) *via* the solution casting method.[187] The high stability of the ether-free skeleton and acid–base interaction (sulfonic acid group and tertiary amine group) greatly improved the structural stability of the membrane, and the Donnan repulsion effect significantly

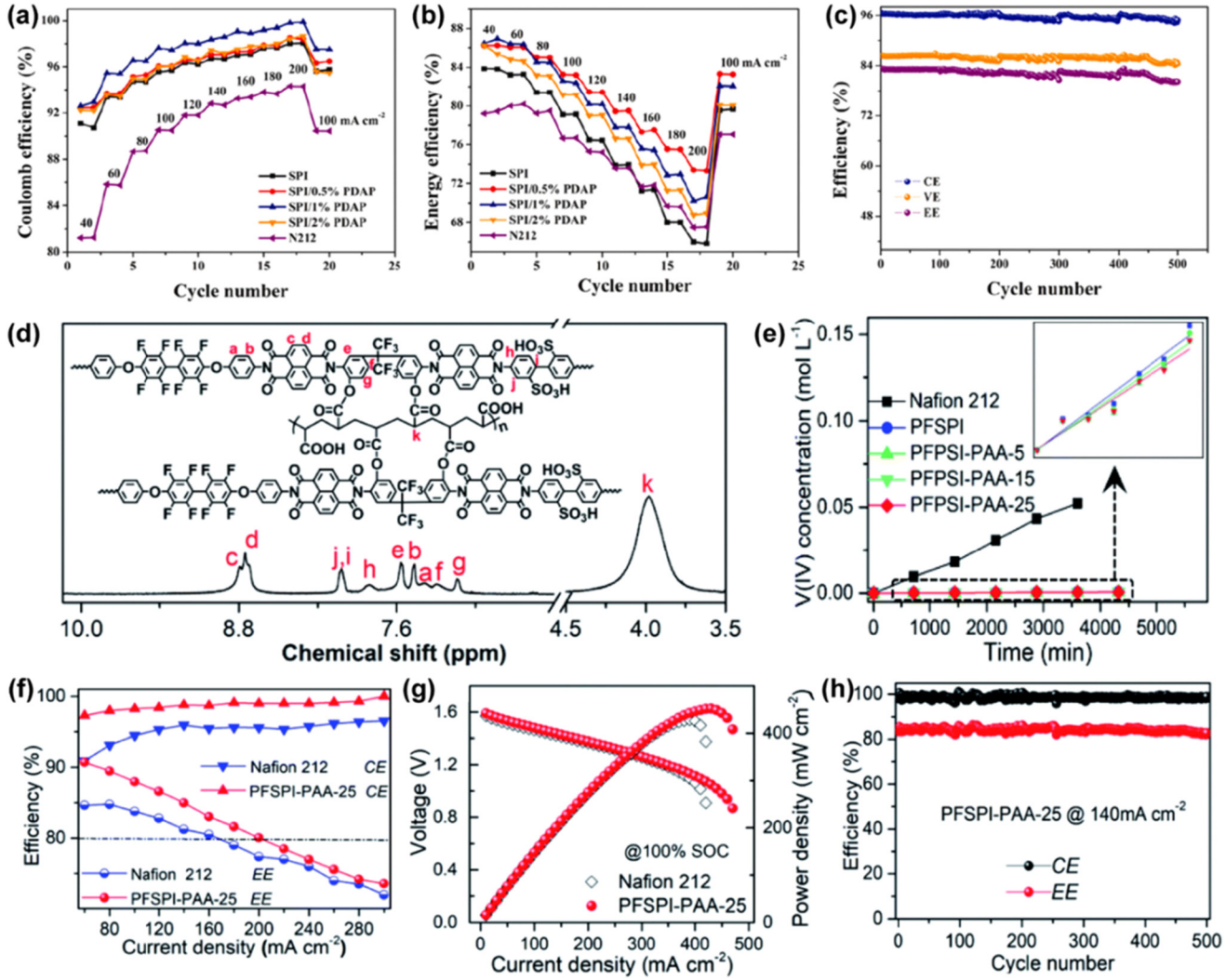

Fig. 16 (a) Coulombic efficiency and (b) energy efficiency of VRFB with different SPI/PDAP and Nafion 212 membranes. (c) Cycling performances of VRFB with SPI/0.5% PDAP membrane at a current density of 100 mA cm^{-2}. Reproduced from ref. 180 with permission from Elsevier, Copyright 2021. (d) ^{1}H NMR spectrum of PFSPI-PAA-25 membrane. (e) Concentration of VO^{2+} across PFSPI, PFSPI-PAA-X and Nafion 212 membranes *versus* time. (f) Coulombic efficiency and energy efficiency of VRFB with different membranes. (g) Polarization curves of VRFB. (h) Efficiencies of VRFB assembled with PFSPI-PAA-25 membrane. Reproduced from ref. 137 with permission from The Royal Society of Chemistry, Copyright 2021.

reduced the permeability of vanadium ions. Compared with the Nafion 212 membrane, the TA15-SPBP membrane showed higher proton conductivity and excellent ion selectivity. The VRFB assembled with the TA15-SPBP membrane showed stable cycling of 1188 times at a current density of 80 mA cm^{-2}, whereas the capacity retention rate of the battery with Nafion 212 was only 11.3% after 200 cycles. Similarly, Pang *et al.* proposed the strategy of synthesizing the side chain of hydroxy bromopropane anion precursor followed by quaternization, forming a polybenzimidazole ionic conductive film with sulfate/quaternary ammonium zwitterion pair ($PBI\text{-}OSO_3^-/OHN^+$).[184] The assembled VRFB exhibited an excellent performance with an coulombic efficiency of 99.2%, energy efficiency of 85.9% and capacity decay rate of 0.31% per cycle. Liao *et al.* prepared a novel fluoro-methyl sulfonated poly(aryl ether ketone) AIEM (60SPAEK-6F-*co*-10% BI).[69] The positively charged benzimidazole group effectively inhibited the crossing of vanadium ions, and the antioxidant C–F bond enhanced the chemical and mechanical stability of the membrane. The VRFB assembled with this AIEM exhibited a higher efficiency than that with Nafion 117 and maintained stable operation for 220 cycles.

Although many AIEMs have been modified by partially fluorinated/non-fluorinated polymers, finding a good balance between high ionic conductivity and dimensional stability is still an important direction for future work. In addition, the durability of AIEMs is also a key factor to be considered because the electrolyte in VRFB has strong acidity and oxidizability. Therefore, the strategies of developing polymer skeletons and new functional groups, as well as optimization of the microphase structure, are promising pathways to obtain high performance AIEMs with strong stability and low cost.

9. Porous membrane

To overcome the disadvantages of high cost and complicated preparation process of the above-mentioned polymer electrolyte membranes, nanofiltration (NF) membranes with a porous structure, which is known as reverse osmosis (RO), were proposed in 1984.[191] The principle of nanofiltration membranes is to prevent the passage of vanadium ions (hydrated) with a larger radius but allow protons with a smaller radius to pass through pore sieving.[77] In 2011, Zhang *et al.* first proposed and designed a polyacrylonitrile (PAN) nanofiltration membrane with an adjustable distribution of pore size for VRFB and then porous membranes for VRFB have attracted considerable attention.[192]

9.1 Design criteria for porous membranes

The migration mechanism of vanadium ions can be divided into three types, namely diffusion, convection, and migration. Zhou *et al.* investigated the transport phenomenon of vanadium ions in porous membranes, and found that the main mechanism for vanadium ion crossover is convection.[193] Reducing the pore size (<15 nm) of membranes can effectively reduce the driving force of convection, but the driving force of migration and diffusion can only be effectively reduced when the pore size is down to the size of vanadium ion (<2 nm). Therefore, reducing the pore size of porous membranes is a feasible method to reduce their permeability. However, the voltage efficiency of the battery will also decrease with a smaller pore size due to the increased ohmic resistance of the film. Thus, to balance the vanadium resistance and ohmic resistance of the membrane, the appropriate pore size of the membrane should be regulated. In addition, the influence of membrane thickness, electrolyte flow rate and other factors should also be considered.

9.2 Methods for the preparation of porous membranes

The methods for preparing porous membranes can be classified into two categories, pore-forming agent and phase inversion. The drying process of the casting solution or the separation process of the pore-forming agents from the matrix can form pores naturally to obtain porous membranes. In the phase inversion method, the solvent and non-solvent diffuse and exchange with each other in a coagulation bath containing polymer, and spontaneously form liquid–liquid phase separation. The polymer-rich phase coagulates to fabricate the membrane body, while the polymer-poor phase forms pores.

The polymer materials for porous membranes include PAN, PVDF, PBI and polyether sulfone (PES) because their ion selectivity is inferior to that of ion exchange membranes, which usually have high vanadium ion permeability. To achieve effective blocking of vanadium species without the loss of too much proton conductivity, previous reports usually adopted organic/inorganic nano-materials filling, grafting and copolymerization, introduction of functional layer, and polymer blending to modify porous membranes.

9.2.1 Organic/inorganic nano-materials filling. A porous polymer filled with organic/inorganic nanomaterials can reduce the pore size and improve the ion selectivity. Zhang *et al.* filled a PAN matrix with SiO_2 nanoparticles by the *in situ* sol–gel process of TEOS to reduce the pore size of the film.[194] This method can effectively improve the ionic selectivity of the membrane and maintain good ionic conductivity. Ling *et al.* also used the sol–gel method to introduce sulfonated silica in the porous PVDF matrix.[195] Pore-filled sulfonated silica can provide a proton transfer carrier and inhibit the permeation of vanadium ions in the membrane.

9.2.2 Grafting and copolymerization. Li *et al.* prepared a hydrophilic porous PSF membrane by grafting sodium *p*-styrene sulfonate (NaSS) on a PSF phase inversion membrane, which was carried out *via* ultraviolet-induced polymerization of vinyl monomer.[196] The grafting degree of the PSF films could be adjusted by controlling the ultraviolet wavelength, photo-initiator concentration and irradiation time. As shown in Fig. 17a, Cao *et al.* also introduced a hydrophilic polyvinylpyrrolidone (PVP) layer on the surface of a PVDF porous membrane through graft polymerization and crosslinking reaction, which improved the overall hydrophilicity of the PVDF membrane and adjusted the pore size distribution.[62] The VRFB assembled with the modified membranes could deliver a coulombic efficiency of 94.4% and energy efficiency of 83.3% at a current density of 80 mA cm^{-2}, which are comparable to that with commercial Nafion 115.

9.2.3 Introducing functional layers/charged groups. Introducing functional layers on the membrane surface is also an effective strategy. Yuan *et al.* used porous PES prepared by the phase inversion method as the carrier, and sprayed zeolite on the top layer to fabricate a composite membrane.[197] As shown in Fig. 17b, the pore size of the zeolite was about 0.5 nm, which is between hydrated vanadium ions (>0.6 nm) and protons (<0.24 nm), and thus the functional top layer perfectly separated vanadium ions from protons. At a current density of 200 mA cm^{-2}, the assembled VRFB exhibited a coulombic efficiency of over 99% and energy efficiency, which is the highest value reported thus far. Chen *et al.* transferred multilayer graphene directly to the surface of a PES porous membrane, which significantly reduced the vanadium crossover in the membrane and increased the proton selectivity.[199] Teng *et al.* also introduced a polypyrrole (PPY) top layer on a porous PES substrate *via* interfacial polymerization, and the composite membrane had lower vanadium ion permeability and area resistance than that with commercial Nafion 115.[200]

To reduce the permeability of vanadium ions, the introduction of charged groups in the polymer membrane substrate is another potential strategy. As shown in Fig. 17c, Zhang *et al.* grafted pyridine groups on chloromethylated polysulfone (CPSF), and formed a positively charged sponge-like structure, which could repel the migration of vanadium ions.[198] In addition, weak bases can further promote protons to pass through the pore wall by acid–base interaction. The cross-

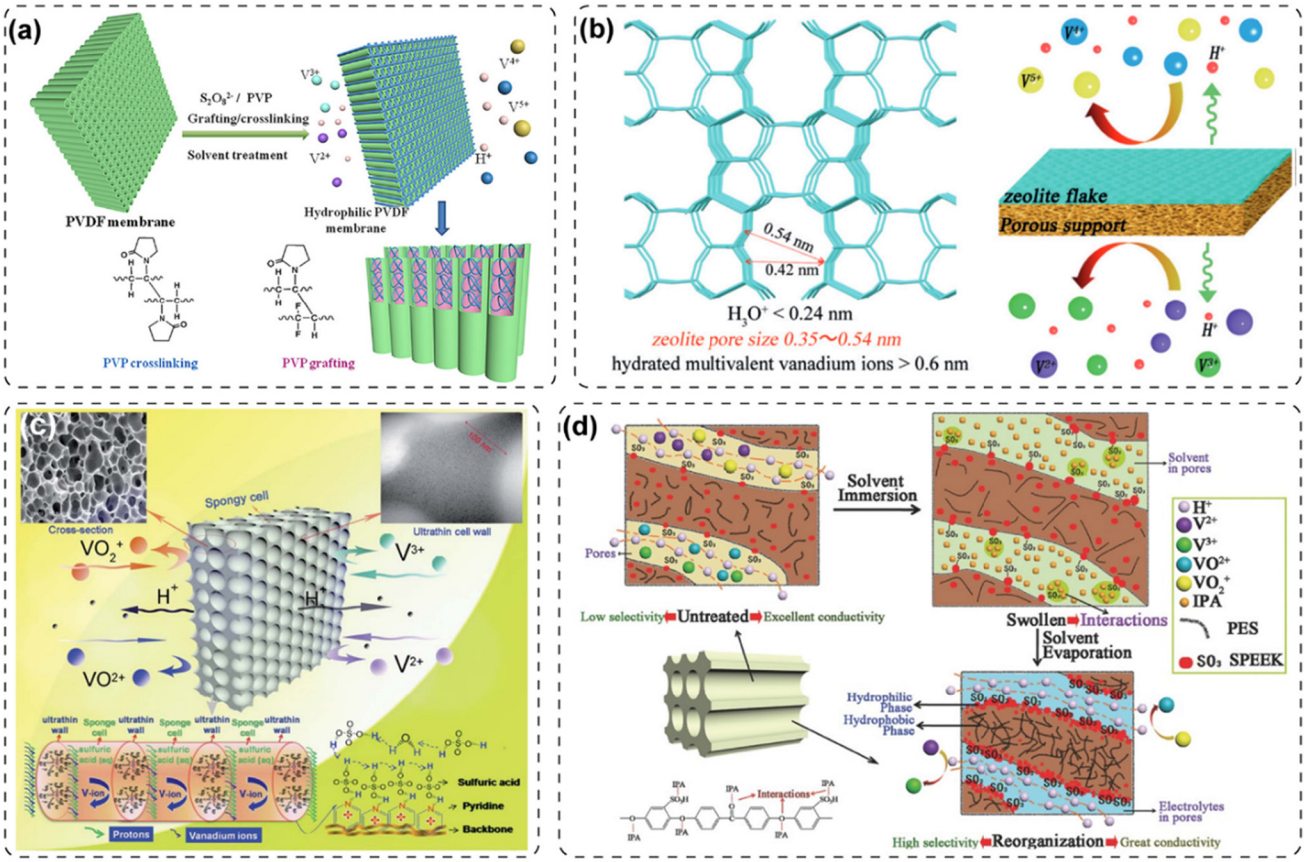

Fig. 17 (a) Hydrophilic ion transport networks and chemical reaction between PVP and PVDF by $K_2S_2O_8$ radical initiation. Reproduced from ref. 62 with permission from Elsevier, Copyright 2015. (b) Design principle of zeolite flake porous membrane for VRFB. Reproduced from ref. 197 with permission from Wiley, Copyright 2016. (c) Designed membranes with symmetric spongy structures in VRFB. Reproduced from ref. 198 with permission from The Royal Society of Chemistry, Copyright 2013. (d) Solvent-induced reorganization of polymer chains in porous PES/SPEEK blended membrane. Reproduced from ref. 77 with permission from Wiley, Copyright 2016.

linking of CPSF with hydrophilic trimethylamine can form a microphase separation structure, which is beneficial for proton conduction. The composite membrane also reduced the cross-crossing of vanadium ions by the Donnan effect and pore size repulsion and the rigid cross-linking network ensured the chemical stability of the membrane.[201] Similarly, the introduction of positively charged imidazole groups on the pore wall of spongy PES or *in situ* polymerization of PPY to obtain a PPY/PES composite film[202] could improve the ion selectivity of membranes.

9.2.4 Inducing the formation of phase separation structures. The process for the formation of a phase separation structure in polymer membranes is difficult to control, and in this case, polymer–solvent interactions provide a method for inducing polymer chain recombination,[203,204] particularly for the formation of unique phase separation structures in hydrophobic/hydrophilic polymer blends. Lu *et al.* introduced isopropanol (IPA) in a PES/SPEEK blend porous membrane to induce the recombination of sulfonated groups, which formed ion transport channels by the interaction between IPA and functional groups in SPEEK.[77] The highly stable hydrophobic porous PES matrix and interconnected pores with hydrophobicity formed a fine phase-separated structure (Fig. 17d), and the assembled VRFB showed a coulombic efficiency of over 99% and energy efficiency of over 91% at a current density of 80 mA cm^{-2}. The control of the pore size and phase separation structure in PES/SPEEK porous composite membranes *via* the selection of different solvents has also been reported in the literatures.[205–207] In addition, Shi *et al.* used hydrophilic polyethylene glycol (PEG 400) to induce the aggregation of SPEEK, resulting in phase separation from the hydrophobic PVDF polymer during the formation of the PVDF/SPEEK porous membrane.[208]

Porous membranes are generally fabricated using polymers with high chemical stability and improved ion selectivity by reducing the transmission channels or introducing charged groups/phase separation structures. Therefore, VRFBs with porous membranes present high coulombic efficiency at low self-discharge rates, but the lower proton conductivity of membranes will cause greater membrane resistance. Therefore, it is necessary to improve the performance of porous membranes to achieve high-performance VRFB.

10. Conclusion and outlook

Flow batteries are considered as the most promising candidates among the numerous large-scale energy storage technologies because of their high reliability, fast response time, long life-time and decoupling of capacity and power. The membrane is one of the key components in flow batteries and its function is to conduct charge carriers and to separate the catholyte from the anolyte in space. Currently, the widely used membrane in flow batteries is perfluorosulfonic acid proton exchange membranes (Nafion) with excellent chemical stability and ionic conductivity. However, their high cost, poor ionic selectivity and low mechanical stability limit their application in VRFB. Tremendous effort has been devoted to the development of polymer electrolyte membranes with enhanced ionic conductivity, long-term durability, and low cost. This review comprehensively summarized the recent research achievements in new membranes in VRFB systems, including CEM, AEM and AIEM, which are charged membranes, and porous membranes.

(1) CEMs are well-developed and widely used membranes in redox flow batteries, and their main challenge is the capacity degradation of the battery systems caused by high vanadium ion permeability. Therefore, previous reports developed multi-scale inorganic material composite membranes and covalent/non-covalent modified organic composite membranes. To reduce the cost of the membrane, new types of CEMs including PTFE, SPEEK, SPI, and PBI have been studied as substitutes for Nafion membranes. These membranes without Nafion exhibit improved ionic selectivity and lower cost, but their poor conductivity and long-term stability need to be improved.

(2) AEMs with cationic groups significantly reduce the permeability of vanadium ions through the membrane but limit the proton conductivity simultaneously, resulting in a lower voltage efficiency. Researchers have regulated the microstructure of membranes by adding inorganic additives, acid treatment and organic modification methods. However, the low redox stability of AEMs still hinders their wide application in VRFB.

(3) To obtain both high ionic conductivity and low vanadium ion crossover, the development of AIEMs has become a major research direction in recent years. However, the methods for the preparation of AIEMs are usually complicated and the distribution of two ion exchange groups in the membrane matrix has limited accuracy, which also hinder their potential application.

(4) In recent years, non-ionic porous membranes based on pore size screening have attracted intense attention in the field of VRFB. To achieve effective blocking effect of vanadium ions without compromising the proton conductivity, it is essential to maintain a hydrophilic pore structure with adjustable pore size. Preparation methods such as filling with organic/inorganic nanomaterials, grafting and copolymerization modification, introducing functional surface layers, and polymer blending have been explored to modify porous membranes. It is worth emphasizing that high-stability and low-cost porous membranes have not been fully achieved for VRFB.

The high cost of membranes has become a bottleneck in the future application of VRFB. Specifically, Nafion membranes are expensive (\$600–800 m^{-2}), whereas several modified non-fluorinated membranes (such as PSF and SPEEK) effectively reduce the membrane cost (\$40 m^{-2}). However, due to the presence of charged functional groups, their chemical stability is generally poor. In contrast, porous membranes greatly reduce the cost of VRFB. Thus, a further cost reduction is the direction that the entire industry needs to focus on.

From the perspective of the structure–activity relationship of modified Nafion membranes, the functionalization of Nafion membranes has become an important strategy. However, Nafion membranes with high vanadium ion permeability are generally used as cation exchange membranes. Alternatively, by doping fillers, their ion transport channels are reduced, and positively charged groups are introduced to build a vanadium barrier, which effectively hinders the cross penetration of vanadium ions. However, the reduction in the number of sulfonic acid groups during the modification process still limits the energy efficiency of VRFB. Therefore, it is still a huge challenge to coordinate the balance between vanadium ion permeability and proton conductivity and reasonably design and prepare advanced modified Nafion membranes with excellent electrochemical properties.

From the perspective of materials science, the performance of membranes is closely related to their microstructure. In many novel ion exchange membranes, the hydrophilic groups responsible for conducting protons and the hydrophobic backbones are arranged arbitrarily, which makes the proton transfer channel unable to effectively transport protons, and even directly leads to dead ends inside the membrane, completely blocking the proton transport channels. In addition to optimizing the composition and polymerization degree of membranes, researchers should also reasonably design their proton channels, constructing more microstructures that are conducive to proton transport but effectively block vanadium ion transport, thus breaking through the constraints of membrane materials, providing support for the wide application of high-performance membranes.

The method for the preparation of membranes also has a significant impact on production costs and future sustainable development. As seen in Table 2, most membranes were prepared *via* the solution casting method, which often requires *N*,*N*-dimethylformamide and *N*,*N*-dimethylacetamide as solvents, leading to potential hazards. In addition, the membranes formed by the polymer blending casting method are mostly composed of petroleum derivatives. Therefore, the development of biopolymers and environmentally friendly solvents is a future trend.

In summary, balancing the selection of material composition, preparation methods, and macro and microstructures is expected to further promote the development of VRFB membranes towards high chemical stability, high ion conductivity, low vanadium permeability, and low cost.

Simultaneously, it is also of great significance for accelerating the commercial application of VRFB and the utilization of clean and renewable energy.

Conflicts of interest

There are no conflicts to declare.

Acknowledgements

This work is supported by National Natural Science Foundation of China (U21B2057) and Chalmers Areas of Advance Materials Science and Energy and Batteries Sweden (BASE).

References

1 J. A. Nieves, A. J. Aristizábal, I. Dyner, O. Báez and D. H. Ospina, Energy demand and greenhouse gas emissions analysis in Colombia: A LEAP model application, *Energy*, 2019, **169**, 380–397.
2 D. Larcher and J.-M. Tarascon, Towards greener and more sustainable batteries for electrical energy storage, *Nat. Chem.*, 2015, **7**, 19–29.
3 J. P. Barton and D. G. Infield, Energy storage and its use with intermittent renewable energy, *IEEE Trans. Energy Convers.*, 2004, **19**, 441–448.
4 Z. Yang, J. Zhang, M. C. W. Kintner-Meyer, X. Lu, D. Choi, J. P. Lemmon and J. Liu, Electrochemical Energy Storage for Green Grid, *Chem. Rev.*, 2011, **111**, 3577–3613.
5 M. Y. Suberu, M. W. Mustafa and N. Bashir, Energy storage systems for renewable energy power sector integration and mitigation of intermittency, *Renewable Sustainable Energy Rev.*, 2014, **35**, 499–514.
6 M. Li, J. Lu, Z. Chen and K. Amine, 30 Years of Lithium-Ion Batteries, *Adv. Mater.*, 2018, **30**, 1800561.
7 V. Di Noto, Electrical Spectroscopy Studies of Lithium and Magnesium Polymer Electrolytes Based on PEG400, *J. Phys. Chem. B*, 2002, **106**, 11139–11154.
8 M. L. Perry and A. Z. Weber, Advanced Redox-Flow Batteries: A Perspective, *J. Electrochem. Soc.*, 2016, **163**, A5064–A5067.
9 C. Zhang, L. Zhang, Y. Ding, S. Peng, X. Guo, Y. Zhao, G. He and G. Yu, Progress and prospects of next-generation redox flow batteries, *Energy Storage Mater.*, 2018, **15**, 324–350.
10 Z. Zhu, T. Jiang, M. Ali, Y. Meng, Y. Jin, Y. Cui and W. Chen, Rechargeable Batteries for Grid Scale Energy Storage, *Chem. Rev.*, 2022, **122**, 16610–16751.
11 H. Prifti, A. Parasuraman, S. Winardi, T. M. Lim and M. Skyllas-Kazacos, Membranes for Redox Flow Battery Applications, *Membranes*, 2012, **2**, 275–306.
12 X. Shi, O. C. Esan, X. Huo, Y. Ma, Z. Pan, L. An and T. S. Zhao, Polymer Electrolyte Membranes for Vanadium Redox Flow Batteries: Fundamentals and Applications, *Prog. Energy Combust. Sci.*, 2021, **85**, 100926.
13 S. Weber, J. F. Peters, M. Baumann and M. Weil, Life Cycle Assessment of a Vanadium Redox Flow Battery, *Environ. Sci. Technol.*, 2018, **52**, 10864–10873.
14 Y. Shi, C. Eze, B. Xiong, W. He, H. Zhang, T. M. Lim, A. Ukil and J. Zhao, Recent development of membrane for vanadium redox flow battery applications: A review, *Appl. Energy*, 2019, **238**, 202–224.
15 M. Skyllas-Kazacos, M. Rychcik, R. G. Robins, A. G. Fane and M. A. Green, New All-Vanadium Redox Flow Cell, *J. Electrochem. Soc.*, 1986, **133**, 1057–1058.
16 G. Kear, A. A. Shah and F. C. Walsh, Development of the all-vanadium redox flow battery for energy storage: a review of technological, financial and policy aspects, *Int. J. Energy Res.*, 2012, **36**, 1105–1120.
17 K. Lourenssen, J. Williams, F. Ahmadpour, R. Clemmer and S. Tasnim, Vanadium redox flow batteries: A comprehensive review, *J. Energy Storage*, 2019, **25**, 100844.
18 K. Zhang, C. Yan and A. Tang, Oxygen-induced electrode activation and modulation essence towards enhanced anode redox chemistry for vanadium flow batteries, *Energy Storage Mater.*, 2021, **34**, 301–310.
19 Y. K. Zeng, T. S. Zhao, L. An, X. L. Zhou and L. Wei, A comparative study of all-vanadium and iron-chromium redox flow batteries for large-scale energy storage, *J. Power Sources*, 2015, **300**, 438–443.
20 H. Zhang and C. Sun, Cost-effective iron-based aqueous redox flow batteries for large-scale energy storage application: A review, *J. Power Sources*, 2021, **493**, 229445.
21 B. Li, Z. Nie, M. Vijayakumar, G. Li, J. Liu, V. Sprenkle and W. Wang, Ambipolar zinc-polyiodide electrolyte for a high-energy density aqueous redox flow battery, *Nat. Commun.*, 2015, **6**, 6303.
22 R. Kim, S. Yuk, J.-H. Lee, C. Choi, S. Kim, J. Heo and H.-T. Kim, Scaling the water cluster size of Nafion membranes for a high performance Zn/Br redox flow battery, *J. Membr. Sci.*, 2018, **564**, 852–858.
23 B. Huskinson, M. P. Marshak, C. Suh, S. Er, M. R. Gerhardt, C. J. Galvin, X. Chen, A. Aspuru-Guzik, R. G. Gordon and M. J. Aziz, A metal-free organic–inorganic aqueous flow battery, *Nature*, 2014, **505**, 195–198.
24 V. Singh, S. Kim, J. Kang and H. R. Byon, Aqueous organic redox flow batteries, *Nano Res.*, 2019, **12**, 1988–2001.
25 W. Yan, G. Qiao, Y. Liu, J. Wei, Z. Tie and Z. Jin, Flexible high-capacity and long-cyclability hydrogel batteries enabled by polyvalent vanadium ion redox chemistry, *J. Power Sources*, 2023, **561**, 232736.
26 L. Zhang, R. Feng, W. Wang and G. Yu, Emerging chemistries and molecular designs for flow batteries, *Nat. Rev. Chem.*, 2022, **6**, 524–543.
27 Y. Liu, G.-H. Wen, J. Liang, S.-S. Bao, J. Wei, H. Wang, P. Zhang, M. Zhu, Q. Jia, J. Ma, L.-M. Zheng and Z. Jin, Aqueous Colloid Flow Batteries Based on Redox-Reversible Polyoxometalate Clusters and Size-Exclusive Membranes, *ACS Energy Lett.*, 2023, **8**, 387–397.

28 B. Jiang, L. Wu, L. Yu, X. Qiu and J. Xi, A comparative study of Nafion series membranes for vanadium redox flow batteries, *J. Membr. Sci.*, 2016, **510**, 18–26.
29 Z. Mai, H. Zhang, X. Li, S. Xiao and H. Zhang, Nafion/polyvinylidene fluoride blend membranes with improved ion selectivity for vanadium redox flow battery application, *J. Power Sources*, 2011, **196**, 5737–5741.
30 Z. Li and Y. Lu, Material Design of Aqueous Redox Flow Batteries: Fundamental Challenges and Mitigation Strategies, *Adv. Mater.*, 2022, **32**, 2002132.
31 T. Mu, W. Tang, N. Shi, G. Wang, T. Wang, T. Wang and J. Yang, Novel ether-free membranes based on poly(p-terphenylene methylimidazole) for vanadium redox flow battery applications, *J. Membr. Sci.*, 2022, **659**, 120793.
32 S.-J. Seo, B.-C. Kim, K.-W. Sung, J. Shim, J.-D. Jeon, K.-H. Shin, S.-H. Shin, S.-H. Yun, J.-Y. Lee and S.-H. Moon, Electrochemical properties of pore-filled anion exchange membranes and their ionic transport phenomena for vanadium redox flow battery applications, *J. Membr. Sci.*, 2013, **428**, 17–23.
33 E. Moukheiber, G. De Moor, L. Flandin and C. Bas, Investigation of ionomer structure through its dependence on ion exchange capacity (IEC), *J. Membr. Sci.*, 2012, **389**, 294–304.
34 D. Chen, S. Wang, M. Xiao and Y. Meng, Synthesis and properties of novel sulfonated poly(arylene ether sulfone) ionomers for vanadium redox flow battery, *Energy Convers. Manage.*, 2010, **51**, 2816–2824.
35 S. S. He and C. W. Frank, Facilitating hydroxide transport in anion exchange membranes via hydrophilic grafts, *J. Mater. Chem. A*, 2014, **2**, 16489–16497.
36 C. Ye, A. Wang, C. Breakwell, R. Tan, C. Grazia Bezzu, E. Hunter-Sellars, D. R. Williams, N. P. Brandon, P. A. A. Klusener, A. R. Kucernak, K. E. Jelfs, N. B. McKeown and Q. Song, Development of efficient aqueous organic redox flow batteries using ion-sieving sulfonated polymer membranes, *Nat. Commun.*, 2022, **13**, 3184.
37 E. Wiedemann, A. Heintz and R. N. Lichtenthaler, Transport properties of vanadium ions in cation exchange membranes: Determination of diffusion coefficients using a dialysis cell, *J. Membr. Sci.*, 1998, **141**, 215–221.
38 J. Chen, B. Wang and J. Yang, Adsorption and Diffusion of VO^{2+} and VO_2^+ across Cation Membrane for All-Vanadium Redox Flow Battery, *Solvent Extr. Ion Exch.*, 2009, **27**, 312–327.
39 R. Tan, A. Wang, R. Malpass-Evans, R. Williams, E. W. Zhao, T. Liu, C. Ye, X. Zhou, B. P. Darwich, Z. Fan, L. Turcani, E. Jackson, L. Chen, S. Y. Chong, T. Li, K. E. Jelfs, A. I. Cooper, N. P. Brandon, C. P. Grey, N. B. McKeown and Q. Song, Hydrophilic microporous membranes for selective ion separation and flow-battery energy storage, *Nat. Mater.*, 2020, **19**, 195–202.
40 J. Wu, C. Yuan, T. Li, Z. Yuan, H. Zhang and X. Li, Dendrite-Free Zinc-Based Battery with High Areal Capacity via the Region-Induced Deposition Effect of Turing Membrane, *J. Am. Chem. Soc.*, 2021, **143**, 13135–13144.
41 H. Zou, Z. Xu, L. Xiong, J. Wang, H. Fu, J. Cao, M. Ding, X. Wang and C. Jia, An alkaline S/Fe redox flow battery endowed with high volumetric-capacity and long cycle-life, *J. Power Sources*, 2024, **591**, 233856.
42 Z. Li, G. Weng, Q. Zou, G. Cong and Y.-C. Lu, A high-energy and low-cost polysulfide/iodide redox flow battery, *Nano Energy*, 2016, **30**, 283–292.
43 J. Ye, S. Yu, C. Zheng, T. Sun, J. Liu and H. Li, Advanced hybrid membrane for vanadium redox flow battery created by polytetrafluoroethylene layer and functionalized silicon carbide nanowires, *Chem. Eng. J.*, 2022, **427**, 131413.
44 S. Maurya, E. Baca, K. K. Bejagam, H. Pratt, T. Anderson, R. Mukundan and C. Fujimoto, Durable and highly selective ion transport of a sulfonated Diels Alder Poly(phenylene) for vanadium redox flow batteries, *J. Power Sources*, 2022, **520**, 230805.
45 X. Lou, B. Lu, M. He, Y. Yu, X. Zhu, F. Peng, C. Qin, M. Ding and C. Jia, Functionalized carbon black modified sulfonated polyether ether ketone membrane for highly stable vanadium redox flow battery, *J. Membr. Sci.*, 2022, **643**, 120015.
46 J. Ye, Y. Cheng, L. Sun, M. Ding, C. Wu, D. Yuan, X. Zhao, C. Xiang and C. Jia, A green SPEEK/lignin composite membrane with high ion selectivity for vanadium redox flow battery, *J. Membr. Sci.*, 2019, **572**, 110–118.
47 X. Teng, J. Dai, J. Su and J. Yin, Modification of Nafion membrane using fluorocarbon surfactant for all vanadium redox flow battery, *J. Membr. Sci.*, 2015, **476**, 20–29.
48 S. Sang, Q. Wu and K. Huang, Preparation of zirconium phosphate (ZrP)/Nafion1135 composite membrane and H^+/VO_2^+ transfer property investigation, *J. Membr. Sci.*, 2007, **305**, 118–124.
49 G.-J. Hwang and H. Ohya, Preparation of cation exchange membrane as a separator for the all-vanadium redox flow battery, *J. Membr. Sci.*, 1996, **120**, 55–67.
50 S. Lu, C. Wu, D. Liang, Q. Tan and Y. Xiang, Layer-by-layer self-assembly of Nafion–[CS–PWA] composite membranes with suppressed vanadium ion crossover for vanadium redox flow battery applications, *RSC Adv.*, 2014, **4**, 24831–24837.
51 L. Ding, X. Song, L. Wang and Z. Zhao, Enhancing proton conductivity of polybenzimidazole membranes by introducing sulfonate for vanadium redox flow batteries applications, *J. Membr. Sci.*, 2019, **578**, 126–135.
52 W. Dai, L. Yu, Z. Li, J. Yan, L. Liu, J. Xi and X. Qiu, Sulfonated Poly(Ether Ether Ketone)/Graphene composite membrane for vanadium redox flow battery, *Electrochim. Acta*, 2014, **132**, 200–207.
53 Y. Xia, X. Hou, X. Chen, F. Mu, Y. Wang, L. Dai, X. Liu, Y. Yu, K. Huang, W. Xing and Z. Xu, Membrane with horizontally rigid zeolite nanosheet arrays against zinc dendrites in zinc-based flow battery, *Chem. Eng. J.*, 2023, **465**, 142912.
54 Y. Zhao, P. Xiang, Y. Wang, X. Sun, D. Cao and H. Zhu, A high ion-conductive and stable porous membrane for neutral aqueous Zn-based flow batteries, *J. Membr. Sci.*, 2021, **640**, 119804.

55 L. Su, D. Zhang, S. Peng, X. Wu, Y. Luo and G. He, Orientated graphene oxide/Nafion ultra-thin layer coated composite membranes for vanadium redox flow battery, *Int. J. Hydrogen Energy*, 2017, **42**, 21806–21816.
56 X. Teng, J. Dai, F. Bi, X. Jiang, Y. Song and G. Yin, Ultra-thin polytetrafluoroethene/Nafion/silica membranes prepared with nano SiO_2 and its comparison with sol-gel derived one for vanadium redox flow battery, *Polym. Sci., Ser. A*, 2015, **280**, 30–36.
57 X. Ling, C. Jia, J. Liu and C. Yan, Preparation and characterization of sulfonated poly(ether sulfone)/sulfonated poly(ether ether ketone) blend membrane for vanadium redox flow battery, *J. Membr. Sci.*, 2012, **415–416**, 306–312.
58 Y. Yao, Z. Wang, Z. Li and Y. Lu, A Dendrite-Free Tin Anode for High-Energy Aqueous Redox Flow Batteries, *Adv. Mater.*, 2021, **33**, 2008095.
59 F. Ai, Z. Wang, N.-C. Lai, Q. Zou, Z. Liang and Y.-C. Lu, Heteropoly acid negolytes for high-power-density aqueous redox flow batteries at low temperatures, *Nat. Energy*, 2022, **7**, 417–426.
60 Y. Shi, Z. Wang, Y. Yao, W. Wang and Y.-C. Lu, High-areal-capacity conversion type iron-based hybrid redox flow batteries, *Energy Environ. Sci.*, 2021, **14**, 6329–6337.
61 S. Kim, T. B. Tighe, B. Schwenzer, J. Yan, J. Zhang, J. Liu, Z. Yang and M. A. Hickner, Chemical and mechanical degradation of sulfonated poly(sulfone) membranes in vanadium redox flow batteries, *J. Appl. Electrochem.*, 2011, **41**, 1201–1213.
62 J. Cao, Z. Yuan, X. Li, W. Xu and H. Zhang, Hydrophilic poly(vinylidene fluoride) porous membrane with well connected ion transport networks for vanadium flow battery, *J. Power Sources*, 2015, **298**, 228–235.
63 F. Wang, Z. Zhang and F. Jiang, Dual-porous structured membrane for ion-selection in vanadium flow battery, *J. Power Sources*, 2021, **506**, 230234.
64 F. Wang, F. Ai and Y.-C. Lu, Ion selective membrane for redox flow battery, what's next?, *Next Energy*, 2023, **1**, 100053.
65 C. Minke and T. Turek, Materials, system designs and modelling approaches in techno-economic assessment of all-vanadium redox flow batteries – A review, *J. Power Sources*, 2018, **376**, 66–81.
66 V. Viswanathan, A. Crawford, D. Stephenson, S. Kim, W. Wang, B. Li, G. Coffey, E. Thomsen, G. Graff, P. Balducci, M. Kintner-Meyer and V. Sprenkle, Cost and performance model for redox flow batteries, *J. Power Sources*, 2014, **247**, 1040–1051.
67 A. Trovò, M. Rugna, N. Poli and M. Guarnieri, Prospects for industrial vanadium flow batteries, *Ceram. Int.*, 2023, **49**, 24487–24498.
68 Q. Wang, Z. G. Qu, Z. Y. Jiang and W. W. Yang, Experimental study on the performance of a vanadium redox flow battery with non-uniformly compressed carbon felt electrode, *Appl. Energy*, 2018, **213**, 293–305.
69 J. B. Liao, M. Z. Lu, Y. Q. Chu and J. L. Wang, Ultra-low vanadium ion diffusion amphoteric ion-exchange membranes for all-vanadium redox flow batteries, *J. Power Sources*, 2015, **282**, 241–247.
70 N. Zhao, A. Platt, H. Riley, R. Qiao, R. Neagu and Z. Shi, Strategy towards high ion selectivity membranes for all-vanadium redox flow batteries, *J. Energy Storage*, 2023, **72**, 108321.
71 Z. Wei, J. Zhao and B. Xiong, Dynamic electro-thermal modeling of all-vanadium redox flow battery with forced cooling strategies, *Appl. Energy*, 2014, **135**, 1–10.
72 X. Yuan, C. Song, A. Platt, N. Zhao, H. Wang, H. Li, K. Fatih and D. Jang, A review of all–vanadium redox flow battery durability: Degradation mechanisms and mitigation strategies, *Int. J. Energy Res.*, 2019, **43**, 6599–6638.
73 J. Ye, X. Zhao, Y. Ma, J. Su, C. Xiang, K. Zhao, M. Ding, C. Jia and L. Sun, Hybrid Membranes Dispersed with Superhydrophilic TiO_2 Nanotubes Toward Ultra-Stable and High-Performance Vanadium Redox Flow Batteries, *Adv. Energy Mater.*, 2020, **10**, 1904041.
74 *Advances in batteries for medium and large-scale energy storage: types and applications*, ed. C. Menictas, M. Skyllas-Kazacos and T. M. Lim, Elsevier, 2014.
75 W. Lu, Z. Yuan, Y. Zhao, H. Zhang, H. Zhang and X. Li, Porous membranes in secondary battery technologies, *Chem. Soc. Rev.*, 2017, **46**, 2199–2236.
76 Q. Luo, L. Li, Z. Nie, W. Wang, X. Wei, B. Li, B. Chen and Z. Yang, *In situ* investigation of vanadium ion transport in redox flow battery, *J. Power Sources*, 2012, **218**, 15–20.
77 W. Lu, Z. Yuan, M. Li, X. Li, H. Zhang and I. Vankelecom, Solvent-Induced Rearrangement of Ion-Transport Channels: A Way to Create Advanced Porous Membranes for Vanadium Flow Batteries, *Adv. Funct. Mater.*, 2017, **27**, 1604587.
78 Y. Zhao, M. Li, Z. Yuan, X. Li, H. Zhang and I. F. J. Vankelecom, Advanced Charged Sponge-Like Membrane with Ultrahigh Stability and Selectivity for Vanadium Flow Batteries, *Adv. Funct. Mater.*, 2016, **26**, 210–218.
79 S. Chae, T. Luo, G. H. Moon, W. Ogieglo, Y. S. Kang and M. Wessling, Ultra-High Proton/Vanadium Selectivity for Hydrophobic Polymer Membranes with Intrinsic Nanopores for Redox Flow Battery, *Adv. Energy Mater.*, 2016, **6**, 1600517.
80 W.-J. Zou, Y.-B. Kim and S. Jung, Capacity fade prediction for vanadium redox flow batteries during long-term operations, *Appl. Energy*, 2024, **356**, 122329.
81 D. Jeong and S. Jung, Numerical analysis of cycling performance of vanadium redox flow battery, *Int. J. Energy Res.*, 2020, **44**, 5209–5222.
82 T. Mohammadi, S. C. Chieng and M. Skyllas Kazacos, Water transport study across commercial ion exchange membranes in the vanadium redox flow battery, *J. Membr. Sci.*, 1997, **133**, 151–159.
83 C. Sun, J. Chen, H. Zhang, X. Han and Q. Luo, Investigations on transfer of water and vanadium ions across Nafion membrane in an operating vanadium redox flow battery, *J. Power Sources*, 2010, **195**, 890–897.

84 W. Y. Hsu and T. D. Gierke, Ion transport and clustering in Nafion perfluorinated membranes, *J. Membr. Sci.*, 1983, **13**, 307–326.
85 T. Xu, Ion exchange membranes: State of their development and perspective, *J. Membr. Sci.*, 2005, **263**, 1–29.
86 A. B. Yaroslavtsev, Perfluorinated ion-exchange membranes, *Polym. Sci., Ser. A*, 2013, **55**, 674–698.
87 *Flow Batteries: From Fundamentals to Applications*, ed. C. Roth, J. Noack and M. Skyllas-Kazacos, John Wiley & Sons, 2022.
88 X. Teng, Y. Zhao, J. Xi, Z. Wu, X. Qiu and L. Chen, Nafion/organic silica modified TiO_2 composite membrane for vanadium redox flow battery via in situ sol–gel reactions, *J. Membr. Sci.*, 2009, **341**, 149–154.
89 C. Sun, A. Zlotorowicz, G. Nawn, E. Negro, F. Bertasi, G. Pagot, K. Vezzù, G. Pace, M. Guarnieri and V. Di Noto, [Nafion/$(WO_3)_x$] hybrid membranes for vanadium redox flow batteries, *Polym. Sci., Ser. A*, 2018, **319**, 110–116.
90 J. Xi, Z. Wu, X. Qiu and L. Chen, Nafion/SiO_2 hybrid membrane for vanadium redox flow battery, *J. Power Sources*, 2007, **166**, 531–536.
91 *60 Years of the Loeb-Sourirajan Membrane: Principles, New Materials, Modelling, Characterization, and Applications*, ed. H. H. Tseng, W. J. Lau, M. A. Al-Ghouti and A. Liang, Elsevier, 2022.
92 C.-H. Lin, M.-C. Yang and H.-J. Wei, Amino-silica modified Nafion membrane for vanadium redox flow battery, *J. Power Sources*, 2015, **282**, 562–571.
93 S.-L. Huang, H.-F. Yu and Y.-S. Lin, Modification of Nafion® Membrane via a Sol-Gel Route for Vanadium Redox Flow Energy Storage Battery Applications, *J. Chem.*, 2017, **2017**, e4590952.
94 X. Teng, J. Lei, X. Gu, J. Dai, Y. Zhu and F. Li, Nafion-sulfonated organosilica composite membrane for all vanadium redox flow battery, *Ionics*, 2012, **18**, 513–521.
95 Md. A. Aziz and S. Shanmugam, Zirconium oxide nanotube–Nafion composite as high performance membrane for all vanadium redox flow battery, *J. Power Sources*, 2012, **18**, 513–521.
96 Md. A. Aziz, D. Han and S. Shanmugam, Ultrahigh Proton/Vanadium Selective and Durable Nafion/$TiZrO_4$ Composite Membrane for High-Performance All-Vanadium Redox Flow Batteries, *ACS Sustainable Chem. Eng.*, 2021, **9**, 11041–11051.
97 C. Wu, S. Lu, J. Zhang and Y. Xiang, Inducing microstructural changes in Nafion by incorporating graphitic carbon nitride to enhance the vanadium-blocking effect, *Phys. Chem. Chem. Phys.*, 2018, **20**, 7694–7700.
98 D. Zhang, Q. Wang, S. Peng, X. Yan, X. Wu and G. He, An interface-strengthened cross-linked graphene oxide/Nafion212 composite membrane for vanadium flow batteries, *J. Membr. Sci.*, 2019, **587**, 117189.
99 Q. Luo, H. Zhang, J. Chen, P. Qian and Y. Zhai, Modification of Nafion membrane using interfacial polymerization for vanadium redox flow battery applications, *J. Membr. Sci.*, 2008, **311**, 98–103.
100 J. Ma, S. Wang, J. Peng, J. Yuan, C. Yu, J. Li, X. Ju and M. Zhai, Covalently incorporating a cationic charged layer onto Nafion membrane by radiation-induced graft copolymerization to reduce vanadium ion crossover, *Eur. Polym. J.*, 2013, **49**, 1832–1840.
101 J. Dai, Y. Dong, C. Yu, Y. Liu and X. Teng, A novel Nafion-g-PSBMA membrane prepared by grafting zwitterionic SBMA onto Nafion via SI-ATRP for vanadium redox flow battery application, *J. Membr. Sci.*, 2018, **554**, 324–330.
102 F. A. Landis and R. B. Moore, Blends of a Perfluorosulfonate Ionomer with Poly(vinylidene fluoride): Effect of Counterion Type on Phase Separation and Crystal Morphology, *Macromolecules*, 2000, **33**, 6031–6041.
103 J.-C. Lin, M. Ouyang, J. M. Fenton, H. R. Kunz, J. T. Koberstein and M. B. Cutlip, Study of blend membranes consisting of Nafion® and vinylidene fluoride–hexafluoropropylene copolymer, *J. Appl. Polym. Sci.*, 1998, **70**, 121–127.
104 X. Teng, C. Sun, J. Dai, H. Liu, J. Su and F. Li, Solution casting Nafion/polytetrafluoroethylene membrane for vanadium redox flow battery application, *Electrochim. Acta*, 2013, **88**, 725–734.
105 X. Teng, J. Dai, J. Su, Y. Zhu, H. Liu and Z. Song, A high performance polytetrafluoroethene/Nafion composite membrane for vanadium redox flow battery application, *J. Power Sources*, 2013, **240**, 131–139.
106 J. grosse Austing, C. Nunes Kirchner, L. Komsiyska and G. Wittstock, Layer-by-layer modification of Nafion membranes for increased life-time and efficiency of vanadium/air redox flow batteries, *J. Membr. Sci.*, 2016, **510**, 259–269.
107 X.-B. Yang, L. Zhao, X.-L. Sui, L.-H. Meng and Z.-B. Wang, Phosphotungstic acid immobilized nanofibers-Nafion composite membrane with low vanadium permeability and high selectivity for vanadium redox flow battery, *J. Colloid Interface Sci.*, 2019, **542**, 177–186.
108 X. Yang, L. Zhao, K. Goh, X. Sui, L. Meng and Z. Wang, Ultra–High Ion Selectivity of a Modified Nafion Composite Membrane for Vanadium Redox Flow Battery by Incorporation of Phosphotungstic Acid Coupled UiO-66-NH_2, *ChemistrySelect*, 2019, **4**, 4633–4641.
109 J. Ye, D. Yuan, M. Ding, Y. Long, T. Long, L. Sun and C. Jia, A cost-effective Nafion/lignin composite membrane with low vanadium ion permeation for high performance vanadium redox flow battery, *J. Power Sources*, 2021, **482**, 229023.
110 Y. Lee, S. Kim, R. Hempelmann, J. H. Jang, H.-J. Kim, J. Han, J. Kim and D. Henkensmeier, Nafion membranes with a sulfonated organic additive for the use in vanadium redox flow batteries, *J. Appl. Polym. Sci.*, 2019, **136**, 47547.
111 X. Teng, J. Dai, F. Bi and G. Yin, Ultra-thin polytetrafluoroethene/Nafion/silica composite membrane with high performance for vanadium redox flow battery, *J. Power Sources*, 2014, **272**, 113–120.

112 J. Ye, J. Liu, C. Zheng, T. Sun, S. Yu and H. Li, Simple acid etched graphene oxide constructing high-performance sandwich structural hybrid membrane for redox flow battery, *Sustainable Mater. Technol.*, 2023, **35**, e00550.

113 X. Teng, C. Yu, X. Wu, Y. Dong, P. Gao, H. Hu, Y. Zhu and J. Dai, PTFE/SPEEK/PDDA/PSS composite membrane for vanadium redox flow battery application, *J. Mater. Sci.*, 2018, **53**, 5204–5215.

114 J. Xi, Z. Li, L. Yu, B. Yin, L. Wang, L. Liu, X. Qiu and L. Chen, Effect of degree of sulfonation and casting solvent on sulfonated poly(ether ether ketone) membrane for vanadium redox flow battery, *J. Power Sources*, 2015, **285**, 195–204.

115 J. Kim, J.-D. Jeon and S.-Y. Kwak, Sulfonated poly(ether ether ketone) composite membranes containing microporous layered silicate AMH-3 for improved membrane performance in vanadium redox flow batteries, *Electrochim. Acta*, 2017, **243**, 220–227.

116 C. Sun, E. Negro, K. Vezzù, G. Pagot, G. Cavinato, A. Nale, Y. Herve Bang and V. Di Noto, Hybrid inorganic-organic proton-conducting membranes based on SPEEK doped with WO_3 nanoparticles for application in vanadium redox flow batteries, *Electrochim. Acta*, 2019, **309**, 311–325.

117 X. Lou, J. Ye, L. Xia, S. Chang, X. Zhao, C. Wu and M. Ding, Highly Efficient and Low Cost SPEEK/TiO_2 Nanocomposite Membrane for Vanadium Redox Flow Battery, *J. Nanosci. Nanotechnol.*, 2019, **19**, 2247–2252.

118 Y. Ji, Z. Y. Tay and S. F. Y. Li, Highly selective sulfonated poly(ether ether ketone)/titanium oxide composite membranes for vanadium redox flow batteries, *J. Membr. Sci.*, 2017, **539**, 197–205.

119 G. Wang, F. Wang, A. Li, M. Zhang, J. Zhang, J. Chen and R. Wang, Sulfonated poly(ether ether ketone)/s–TiO_2 composite membrane for a vanadium redox flow battery, *J. Appl. Polym. Sci.*, 2020, **137**, 48830.

120 X. M. Myures, S. Suresh and G. Arthanareeswaran, Construction of thermal, chemical and mechanically stable ion exchange membranes with improved ion selectivity for vanadium redox flow batteries applications, *J. Power Sources*, 2024, **591**, 233818.

121 W. Dai, Y. Shen, Z. Li, L. Yu, J. Xi and X. Qiu, SPEEK/Graphene oxide nanocomposite membranes with superior cyclability for highly efficient vanadium redox flow battery, *J. Mater. Chem. A*, 2014, **2**, 12423–12432.

122 L. Zheng, H. Wang, R. Niu, Y. Zhang and H. Shi, Sulfonated poly(ether ether ketone)/sulfonated graphene oxide hybrid membrane for vanadium redox flow battery, *Electrochim. Acta*, 2018, **282**, 437–447.

123 C. Jia, Y. Cheng, X. Ling, G. Wei, J. Liu and C. Yan, Sulfonated Poly(Ether Ether Ketone)/Functionalized Carbon Nanotube Composite Membrane for Vanadium Redox Flow Battery Applications, *Electrochim. Acta*, 2015, **153**, 44–48.

124 M. Ding, X. Ling, D. Yuan, Y. Cheng, C. Wu, Z.-S. Chao, L. Sun, C. Yan and C. Jia, SPEEK Membrane of Ultrahigh Stability Enhanced by Functionalized Carbon Nanotubes for Vanadium Redox Flow Battery, *Front. Chem.*, 2018, **6**, 286.

125 L. Yu and J. Xi, Durable and Efficient PTFE Sandwiched SPEEK Membrane for Vanadium Flow Batteries, *ACS Appl. Mater. Interfaces*, 2016, **8**, 23425–23430.

126 L. Zhao, F. Li, Y. Guo, Y. Dong, J. Liu, Y. Wang, J. Kang, G. Zhou and Q. Liu, SPEEK/PVDF binary membrane as an alternative proton-exchange membrane in vanadium redox flow battery application, *High Perform. Polym.*, 2017, **29**, 127–132.

127 J. Xi, W. Dai and L. Yu, Polydopamine coated SPEEK membrane for a vanadium redox flow battery, *RSC Adv.*, 2015, **5**, 33400–33406.

128 W. Wei, H. Zhang, X. Li, Z. Mai and H. Zhang, Poly (tetrafluoroethylene) reinforced sulfonated poly(ether ether ketone) membranes for vanadium redox flow battery application, *J. Power Sources*, 2012, **208**, 421–425.

129 J. Li, Y. Zhang and L. Wang, Preparation and characterization of sulfonated polyimide/TiO_2 composite membrane for vanadium redox flow battery, *J. Solid State Electrochem.*, 2014, **18**, 729–737.

130 J. Li, Y. Zhang, S. Zhang, X. Huang and L. Wang, Novel sulfonated polyimide/ZrO_2 composite membrane as a separator of vanadium redox flow battery, *Polym. Adv. Technol.*, 2014, **25**, 1610–1615.

131 Y. Zhang, J. Li, L. Wang and S. Zhang, Sulfonated polyimide/AlOOH composite membranes with decreased vanadium permeability and increased stability for vanadium redox flow battery, *J. Solid State Electrochem.*, 2014, **18**, 3479–3490.

132 J. Li, Y. Zhang, S. Zhang and X. Huang, Sulfonated polyimide/s-MoS_2 composite membrane with high proton selectivity and good stability for vanadium redox flow battery, *J. Membr. Sci.*, 2015, **490**, 179–189.

133 J. Liu, H. Duan, W. Xu, J. Long, W. Huang, H. Luo, J. Li and Y. Zhang, Branched sulfonated polyimide/s-MWCNTs composite membranes for vanadium redox flow battery application, *Int. J. Hydrogen Energy*, 2021, **46**, 34767–34776.

134 M. Yue, Y. Zhang and L. Wang, Sulfonated polyimide/chitosan composite membrane for vanadium redox flow battery: Influence of the infiltration time with chitosan solution, *Polym. Sci., Ser. A*, 2012, **217**, 6–12.

135 M. Yue, Y. Zhang and L. Wang, Sulfonated polyimide/chitosan composite membrane for vanadium redox flow battery: Membrane preparation, characterization, and single cell performance, *J. Appl. Polym. Sci.*, 2013, **127**, 4150–4159.

136 X. Huang, S. Zhang, Y. Zhang, H. Zhang and X. Yang, Sulfonated polyimide/chitosan composite membranes for a vanadium redox flow battery: influence of the sulfonation degree of the sulfonated polyimide, *Polym. J.*, 2016, **48**, 905–918.

137 J. Li, W. Xu, W. Huang, J. Long, J. Liu, H. Luo, Y. Zhang and L. Chu, Stable covalent cross-linked polyfluoro sulfonated polyimide membranes with high proton conductance and vanadium resistance for application in vanadium redox flow batteries, *J. Mater. Chem. A*, 2021, **9**, 24704–24711.

138 S. Liu, L. Wang, B. Zhang, B. Liu, J. Wang and Y. Song, Novel sulfonated polyimide/polyvinyl alcohol blend membranes for vanadium redox flow battery applications, *J. Mater. Chem. A*, 2015, **3**, 2072–2081.

139 H. Yu, Y. Xia, H. Zhang and Y. Wang, Preparation of sulfonated polyimide/polyvinyl alcohol composite membrane for vanadium redox flow battery applications, *Polym. Bull.*, 2021, **78**, 4183–4204.

140 J. Li, H. Li, H. Duan, J. Long, W. Huang, Y. Yu, W. Zhu, L. Chen, J. Chen and Y. Zhang, Sulfonated polyimide membranes with branched architecture and unique diamine monomer for implementation in vanadium redox flow battery, *J. Power Sources*, 2024, **591**, 233892.

141 J. Li, S. Liu, Z. He and Z. Zhou, A novel branched side-chain-type sulfonated polyimide membrane with flexible sulfoalkyl pendants and trifluoromethyl groups for vanadium redox flow batteries, *J. Power Sources*, 2017, **347**, 114–126.

142 K. Y. Wang, Y. Xiao and T.-S. Chung, Chemically modified polybenzimidazole nanofiltration membrane for the separation of electrolytes and cephalexin, *Chem. Eng. Sci.*, 2006, **61**, 5807–5817.

143 K. Y. Wang and T.-S. Chung, Fabrication of polybenzimidazole (PBI) nanofiltration hollow fiber membranes for removal of chromate, *J. Membr. Sci.*, 2006, **281**, 307–315.

144 J.-H. Kim, H.-J. Kim, T.-H. Lim and H.-I. Lee, Dependence of the performance of a high-temperature polymer electrolyte fuel cell on phosphoric acid-doped polybenzimidazole ionomer content in cathode catalyst layer, *J. Power Sources*, 2007, **170**, 275–280.

145 L. Ding and L. Wang, Preparation of novel structure polybenzimidazole with thiophene ring for high performance proton conducting membrane in vanadium flow battery, *J. Power Sources*, 2023, **564**, 232858.

146 D. Chen, H. Qi, T. Sun, C. Yan, Y. He, C. Kang, Z. Yuan and X. Li, Polybenzimidazole membrane with dual proton transport channels for vanadium flow battery applications, *J. Membr. Sci.*, 2019, **586**, 202–210.

147 C. Noh, M. Jung, D. Henkensmeier, S. W. Nam and Y. Kwon, Vanadium Redox Flow Batteries Using meta-Polybenzimidazole-Based Membranes of Different Thicknesses, *ACS Appl. Mater. Interfaces*, 2017, **9**, 36799–36809.

148 Y. H. Wan, J. Sun, H. R. Jiang, X. Z. Fan and T. S. Zhao, A highly-efficient composite polybenzimidazole membrane for vanadium redox flow battery, *J. Power Sources*, 2021, **489**, 229502.

149 N. Wang, S. Peng, H. Wang, Y. Li, S. Liu and Y. Liu, SPPEK/WO_3 hybrid membrane fabricated via hydrothermal method for vanadium redox flow battery, *Electrochem. Commun.*, 2012, **17**, 30–33.

150 N. Wang, J. Yu, Z. Zhou, D. Fang, S. Liu and Y. Liu, SPPEK/TPA composite membrane as a separator of vanadium redox flow battery, *J. Membr. Sci.*, 2013, **437**, 114–121.

151 L. Chen, S. Zhang, Y. Chen and X. Jian, Low vanadium ion permeabilities of sulfonated poly(phthalazinone ether ketone)s provide high efficiency and stability for vanadium redox flow batteries, *J. Power Sources*, 2017, **355**, 23–30.

152 F. Wei and J. Yang, Sulfonated poly(ether sulfone)/short-carboxylic multi-walled carbon nanotube composite membrane applied for vanadium redox flow battery, *High Perform. Polym.*, 2019, **31**, 304–309.

153 J. Xie, G. Li and W. Tan, Preparation and characterization of SPES/PVA (double-layer) membrane for vanadium redox flow battery, *High Perform. Polym.*, 2019, **31**, 148–153.

154 Y. Zhang, X. Zhou, R. Xue, Q. Yu, F. Jiang and Y. Zhong, Proton exchange membranes with ultra-low vanadium ions permeability improved by sulfated zirconia for all vanadium redox flow battery, *Int. J. Hydrogen Energy*, 2019, **44**, 5997–6006.

155 Y. Zhang, Y. Zhong, W. Bian, W. Liao, X. Zhou and F. Jiang, Robust proton exchange membrane for vanadium redox flow batteries reinforced by silica-encapsulated nanocellulose, *Int. J. Hydrogen Energy*, 2020, **45**, 9803–9810.

156 B. Yin, Z. Li, W. Dai, L. Wang, L. Yu and J. Xi, Highly branched sulfonated poly(fluorenyl ether ketone sulfone)s membrane for energy efficient vanadium redox flow battery, *J. Power Sources*, 2015, **285**, 109–118.

157 X. Li, Y. Yu and Y. Meng, Novel Quaternized Poly(arylene ether sulfone)/Nano-ZrO_2 Composite Anion Exchange Membranes for Alkaline Fuel Cells, *ACS Appl. Mater. Interfaces*, 2013, **5**, 1414–1422.

158 K. Leung, Q. Xu, T. S. Zhao, L. Zeng and C. Zhang, Preparation of silica nanocomposite anion-exchange membranes with low vanadium-ion crossover for vanadium redox flow batteries, *Electrochim. Acta*, 2013, **105**, 584–592.

159 B. Zhang, M. Zhao, Q. Liu, X. Zhang, Y. Fu, E. Zhang, G. Wang, Z. Zhang and S. Zhang, Advanced anion exchange membranes with selective swelling-induced ion transport channels for vanadium flow battery application, *J. Membr. Sci.*, 2022, **642**, 119985.

160 T. Ban, M. Guo, Y. Wang, J. Ma, X. Wang, Z. Wang and X. Zhu, Efficient and durable vanadium flow batteries enabled by high-performance fluorinated poly(aryl piperidinium) membranes, *J. Mater. Chem. A*, 2023, **11**, 24013–24025.

161 G. Shukla and V. K. Shahi, Amine functionalized graphene oxide containing C16 chain grafted with poly(ether sulfone) by DABCO coupling: Anion exchange membrane for vanadium redox flow battery, *J. Membr. Sci.*, 2019, **575**, 109–117.

162 Y. Xing, K. Geng, X. Chu, C. Wang, L. Liu and N. Li, Chemically stable anion exchange membranes based on C2-Protected imidazolium cations for vanadium flow battery, *J. Membr. Sci.*, 2021, **618**, 118696.

163 X. Ren, L. Zhao, X. Che, Y. Cai, Y. Li, H. Li, H. Chen, H. He, J. Liu and J. Yang, Quaternary ammonium groups

grafted polybenzimidazole membranes for vanadium redox flow battery applications, *J. Power Sources*, 2020, **457**, 228037.

164 Y. Du, L. Gao, L. Hu, M. Di, X. Yan, B. An and G. He, The synergistic effect of protonated imidazole-hydroxyl-quaternary ammonium on improving performances of anion exchange membrane assembled flow batteries, *J. Membr. Sci.*, 2020, **603**, 118011.

165 J.-K. Jang, S.-W. Jo, J. W. Jeon, B. G. Kim, S. J. Yoon, D. M. Yu, Y. T. Hong, H.-T. Kim and T.-H. Kim, Alkyl Spacer Grafted ABPBI Membranes with Enhanced Acid-Absorption Capabilities for Use in Vanadium Redox Flow Batteries, *ACS Appl. Energy Mater.*, 2021, **4**, 4672–4685.

166 Z. Tao, C. Wang, S. Cai, J. Qian and J. Li, Efficiency and Oxidation Performance of Densely Flexible Side-Chain Piperidinium-Functionalized Anion Exchange Membranes for Vanadium Redox Flow Batteries, *ACS Appl. Energy Mater.*, 2021, **4**, 14488–14496.

167 S. Maurya, S.-H. Shin, K.-W. Sung and S.-H. Moon, Anion exchange membrane prepared from simultaneous polymerization and quaternization of 4-vinyl pyridine for non-aqueous vanadium redox flow battery applications, *J. Power Sources*, 2014, **255**, 325–334.

168 Y. Ma, L. Li, L. Ma, N. A. Qaisrani, S. Gong, P. Li, F. Zhang and G. He, Cyclodextrin templated nanoporous anion exchange membrane for vanadium flow battery application, *J. Membr. Sci.*, 2019, **586**, 98–105.

169 Y. Ma, N. A. Qaisrani, L. Ma, P. Li, L. Li, S. Gong, F. Zhang and G. He, Side chain hydrolysis method to prepare nanoporous membranes for vanadium flow battery application, *J. Membr. Sci.*, 2018, **560**, 67–76.

170 M. Abdiani, E. Abouzari-Lotf, T. M. Ting, P. M. Nia, S. S. Sha'rani, A. Shockravi and A. Ahmad, Novel polyolefin based alkaline polymer electrolyte membrane for vanadium redox flow batteries, *J. Power Sources*, 2019, **424**, 245–253.

171 L. Liu, C. Wang, Z. He, R. Das, B. Dong, X. Xie and Z. Guo, An overview of amphoteric ion exchange membranes for vanadium redox flow batteries, *J. Mater. Sci. Technol.*, 2021, **69**, 212–227.

172 G. Hu, Y. Wang, J. Ma, J. Qiu, J. Peng, J. Li and M. Zhai, A novel amphoteric ion exchange membrane synthesized by radiation-induced grafting α-methylstyrene and N, N-dimethylaminoethyl methacrylate for vanadium redox flow battery application, *J. Membr. Sci.*, 2012, **407–408**, 184–192.

173 M. S. Lee, H. G. Kang, J. D. Jeon, Y. W. Choi and Y. G. Yoon, A novel amphoteric ion-exchange membrane prepared by the pore-filling technique for vanadium redox flow batteries, *RSC Adv.*, 2016, **6**, 63023–63029.

174 J. Qiu, J. Zhang, J. Chen, J. Peng, L. Xu, M. Zhai, J. Li and G. Wei, Amphoteric ion exchange membrane synthesized by radiation-induced graft copolymerization of styrene and dimethylaminoethyl methacrylate into PVDF film for vanadium redox flow battery applications, *J. Membr. Sci.*, 2009, **334**, 9–15.

175 Y. Cui, X. Chen, Y. Wang, J. Peng, L. Zhao, J. Du and M. Zhai, Amphoteric Ion Exchange Membranes Prepared by Preirradiation-Induced Emulsion Graft Copolymerization for Vanadium Redox Flow Battery, *Polymers*, 2019, **11**, 1482.

176 J. Ma, Y. Wang, J. Peng, J. Qiu, L. Xu, J. Li and M. Zhai, Designing a new process to prepare amphoteric ion exchange membrane with well-distributed grafted chains for vanadium redox flow battery, *J. Membr. Sci.*, 2012, **419–420**, 1–8.

177 J. Qiu, M. Zhai, J. Chen, Y. Wang, J. Peng, L. Xu, J. Li and G. Wei, Performance of vanadium redox flow battery with a novel amphoteric ion exchange membrane synthesized by two-step grafting method, *J. Membr. Sci.*, 2009, **342**, 215–220.

178 D. Chen and X. Li, Sulfonated poly(ether ether ketone) membranes containing pendent carboxylic acid groups and their application in vanadium flow battery, *J. Power Sources*, 2014, **247**, 629–635.

179 H.-Y. Jung, M.-S. Cho, T. Sadhasivam, J.-Y. Kim, S.-H. Roh and Y. Kwon, High ionic selectivity of low permeable organic composite membrane with amphiphilic polymer for vanadium redox flow batteries, *Polym. Sci., Ser. A*, 2018, **324**, 69–76.

180 M. Zhang, G. Wang, F. Li, Z. He, J. Zhang, J. Chen and R. Wang, High conductivity membrane containing polyphosphazene derivatives for vanadium redox flow battery, *J. Membr. Sci.*, 2021, **630**, 119322.

181 L. Cao, Q. Sun, Y. Gao, L. Liu and H. Shi, Novel acid-base hybrid membrane based on amine-functionalized reduced graphene oxide and sulfonated polyimide for vanadium redox flow battery, *Electrochim. Acta*, 2015, **158**, 24–34.

182 Y. Zhang, S. Zhang, X. Huang, Y. Zhou, Y. Pu and H. Zhang, Synthesis and properties of branched sulfonated polyimides for membranes in vanadium redox flow battery application, *Electrochim. Acta*, 2016, **210**, 308–320.

183 J. Dai, Y. Dong, P. Gao, J. Ren, C. Yu, H. Hu, Y. Zhu and X. Teng, A sandwiched bipolar membrane for all vanadium redox flow battery with high coulombic efficiency, *Polymer*, 2018, **140**, 233–239.

184 B. Pang, X. Wu, Y. Guo, M. Yang, R. Du, W. Chen, X. Yan, F. Cui and G. He, Anionic conductive group tunable amphoteric polybenzimidazole ion conductive membrane for vanadium redox flow battery, *J. Membr. Sci.*, 2023, **670**, 121351.

185 S. Kumar, M. Bhushan and V. K. Shahi, Cross-linked amphoteric membrane: Sulphonated poly(ether ether ketone) grafted with 2,4,6-tris(dimethylaminomethyl) phenol using functionalized side chain spacers for vanadium redox flow battery, *J. Power Sources*, 2020, **448**, 227358.

186 J. Liao, Y. Chu, Q. Zhang, K. Wu, J. Tang, M. Lu and J. Wang, Fluoro-methyl sulfonated poly(arylene ether ketone-co-benzimidazole) amphoteric ion-exchange mem-

branes for vanadium redox flow battery, *Electrochim. Acta*, 2017, **258**, 360–370.

187 J. Xu, S. Dong, P. Li, W. Li, F. Tian, J. Wang, Q. Cheng, Z. Yue and H. Yang, Novel ether-free sulfonated poly (biphenyl) tethered with tertiary amine groups as highly stable amphoteric ionic exchange membranes for vanadium redox flow battery, *Chem. Eng. J.*, 2021, **424**, 130314.

188 Y. Chen, S. Zhang, J. Jin, C. Liu, Q. Liu and X. Jian, Poly (phthalazinone ether ketone) Amphoteric Ion Exchange Membranes with Low Water Transport and Vanadium Permeability for Vanadium Redox Flow Battery Application, *ACS Appl. Energy Mater.*, 2019, **2**, 8207–8218.

189 C.-P. Li, S.-M. Zhang, S.-B. Wang, X.-F. Xie and C.-S. Deng, Study of Chemical Modified Amphoteric Ion Exchange Membrane from Taurine, *ECS Electrochem. Lett.*, 2014, **3**, A102–A104.

190 Y. Chen, S. Zhang, Q. Liu and X. Jian, The effect of counter-ion substitution on poly(phthalazinone ether ketone) amphoteric ion exchange membranes for vanadium redox flow battery, *J. Membr. Sci.*, 2021, **620**, 118816.

191 P. Vandezande, L. E. M. Gevers and I. F. J. Vankelecom, Solvent resistant nanofiltration: separating on a molecular level, *Chem. Soc. Rev.*, 2008, **37**, 365–405.

192 H. Zhang, H. Zhang, X. Li, Z. Mai and J. Zhang, Nanofiltration (NF) membranes: The next generation separators for all vanadium redox flow batteries (VRBs)?, *Energy Environ. Sci.*, 2011, **4**, 1676–1679.

193 X. L. Zhou, T. S. Zhao, L. An, Y. K. Zeng and L. Wei, Modeling of ion transport through a porous separator in vanadium redox flow batteries, *J. Power Sources*, 2016, **327**, 67–76.

194 H. Zhang, H. Zhang, X. Li, Z. Mai and W. Wei, Silica modified nanofiltration membranes with improved selectivity for redox flow battery application, *Energy Environ. Sci.*, 2012, **5**, 6299–6303.

195 L. Ling, M. Xiao, D. Han, S. Ren, S. Wang and Y. Meng, Porous composite membrane of PVDF/Sulfonic silica with high ion selectivity for vanadium redox flow battery, *J. Membr. Sci.*, 2019, **585**, 230–237.

196 Y. Li, H. Zhang, H. Zhang, J. Cao, W. Xu and X. Li, Hydrophilic porous poly(sulfone) membranes modified by UV-initiated polymerization for vanadium flow battery application, *J. Membr. Sci.*, 2014, **454**, 478–487.

197 Z. Yuan, X. Zhu, M. Li, W. Lu, X. Li and H. Zhang, A Highly Ion-Selective Zeolite Flake Layer on Porous Membranes for Flow Battery Applications, *Angew. Chem., Int. Ed.*, 2016, **55**, 3058–3062.

198 H. Zhang, H. Zhang, F. Zhang, X. Li, Y. Li and I. Vankelecom, Advanced charged membranes with highly symmetric spongy structures for vanadium flow battery application, *Energy Environ. Sci.*, 2013, **6**, 776–781.

199 Q. Chen, Y.-Y. Du, K.-M. Li, H.-F. Xiao, W. Wang and W.-M. Zhang, Graphene enhances the proton selectivity of porous membrane in vanadium flow batteries, *Mater. Des.*, 2017, **113**, 149–156.

200 X. Teng, M. Wang, G. Li and J. Dai, Polypyrrole thin film composite membrane prepared via interfacial polymerization with high selectivity for vanadium redox flow battery, *React. Funct. Polym.*, 2020, **157**, 104777.

201 Y. Zhao, H. Zhang, C. Xiao, L. Qiao, Q. Fu and X. Li, Highly selective charged porous membranes with improved ion conductivity, *Nano Energy*, 2018, **48**, 353–360.

202 Z. Yuan, Q. Dai, Y. Zhao, W. Lu, X. Li and H. Zhang, Polypyrrole modified porous poly(ether sulfone) membranes with high performance for vanadium flow batteries, *J. Mater. Chem. A*, 2016, **4**, 12955–12962.

203 M. A. Alaei Shahmirzadi, S. S. Hosseini, G. Ruan and N. R. Tan, Tailoring PES nanofiltration membranes through systematic investigations of prominent design, fabrication and operational parameters, *RSC Adv.*, 2015, **5**, 49080–49097.

204 W. Lu, H. Zhang and X. Li, Membranes Fabricated by Solvent treatment for Flow Battery: Effects of initial structures and intrinsic properties, *J. Membr. Sci.*, 2019, **577**, 212–218.

205 L. Qiao, H. Zhang, W. Lu, C. Xiao, Q. Fu, X. Li and I. F. J. Vankelecom, Advanced porous membranes with slit-like selective layer for flow battery, *Nano Energy*, 2018, **54**, 73–81.

206 H. Zhang, C. Ding, J. Cao, W. Xu, X. Li and H. Zhang, A novel solvent-template method to manufacture nano-scale porous membranes for vanadium flow battery applications, *J. Mater. Chem. A*, 2014, **2**, 9524–9531.

207 D. Chen, D. Li and X. Li, Hierarchical porous poly (ether sulfone) membranes with excellent capacity retention for vanadium flow battery application, *J. Power Sources*, 2017, **353**, 11–18.

208 D. Shi, C. Li, Z. Yuan and G. Li, Soft Template-Induced Porous Polyvinylidene Fluoride Membrane for Vanadium Flow Batteries, *Trans. Tianjin Univ.*, 2023, **29**, 284–292.